Accepted for publication in *Nature* published by SpringerNature. The published version is available at: https://doi.org/10.1038/s41586-018-0563-7

Plant functional trait change across a warming tundra biome

Anne D. Bjorkman[1,2,3*], Isla H. Myers-Smith[2], Sarah C. Elmendorf[4,5], Signe Normand[1,6,7], Nadja Rüger[8,9], Pieter S.A. Beck[10], Anne Blach-Overgaard[1,7], Daan Blok[11], J. Hans C. Cornelissen[12], Bruce C. Forbes[13], Damien Georges[14,2], Scott J. Goetz[15], Kevin Guay[16], Gregory H.R. Henry[17], Janneke HilleRisLambers[18], Robert D. Hollister[19], Dirk N. Karger[20], Jens Kattge[21,8], Peter Manning[3], Janet S. Prevéy[22], Christian Rixen[22], Gabriela Schaepman-Strub[23], Haydn J.D. Thomas[2], Mark Vellend[24], Martin Wilmking[25], Sonja Wipf[22], Michele Carbognani[26], Luise Hermanutz[27], Esther Levesque[28], Ulf Molau[29], Alessandro Petraglia[26], Nadejda A. Soudzilovskaia[30], Marko Spasojevic[31], Marcello Tomaselli[26], Tage Vowles[32], Juha M. Alatalo[33], Heather Alexander[34], Alba Anadon-Rosell[35,36], Sandra Angers-Blondin[2], Mariska te Beest[37,38], Logan Berner[15], Robert G. Björk[32], Agata Buchwal[39,40], Allan Buras[41], Katie Christie[42], Laura S Collier[27], Elisabeth J. Cooper[43], Stefan Dullinger[44], Bo Elberling[45], Anu Eskelinen[46,8,47], Esther R. Frei[17,20], Maitane Iturrate Garcia[23], Oriol Grau[48,49], Paul Grogan[50], Martin Hallinger[51], Karen A. Harper[52], Monique M.P.D. Heijmans[53], James Hudson[54], Karl Hülber[44], Colleen M. Iversen[55], Francesca Jaroszynska[56,22], Jill Johnstone[57], Rasmus Halfdan Jorgensen[58], Elina Kaarlejärvi[37,59], Rebecca Klady[60], Sara Kuleza[57], Aino Kulonen[22], Laurent J. Lamarque[28], Trevor Lantz[61], Chelsea J. Little[23,62], James David Mervyn Speed[63], Anders Michelsen[64,65], Ann Milbau[66], Jacob Nabe-Nielsen[67], Sigrid Schøler Nielsen[1], Josep M. Ninot[35,36], Steve Oberbauer[68], Johan Olofsson[37], Vladimir G. Onipchenko[69], Sabine B. Rumpf[44], Philipp Semenchuk[43], Rohan Shetti[25], Lorna E. Street[2], Katharine Suding[4], Ken D. Tape[70], Andrew Trant[71], Urs Treier[1], Jean-Pierre Tremblay[72], Maxime Tremblay[28], Susanna Venn[73], Stef Weijers[74], Tara Zamin[50], Noemie Boulanger-Lapointe[17], William A. Gould[75], Dave Hik[76], Annika Hofgaard[77], Ingibjörg Svala Jónsdóttir[78,79], Janet Jorgenson[80], Julia Klein[81], Borgthor Magnusson[82], Craig Tweedie[83], Philip A. Wookey[84], Michael Bahn[85], Benjamin Blonder[86,87], Peter van Bodegom[88], Benjamin Bond-Lamberty[89], Giandiego Campetella[90], Bruno E.L. Cerabolini[91], F. Stuart Chapin III[92], Will Cornwell[93], Joseph Craine[94], Matteo Dainese[95], Franciska T. de Vries[96], Sandra Díaz[97], Brian J. Enquist[98,99], Walton Green[100], Ruben Milla[101], Ülo Niinemets[102], Yusuke Onoda[103], Jenny Ordonez[104], Wim A. Ozinga[105,106], Josep Penuelas[107,49], Hendrik Poorter[108], Peter Poschlod[109], Peter B. Reich[110,111], Brody Sandel[112], Brandon Schamp[113], Serge Sheremetev[114], Evan Weiher[115]

1. Ecoinformatics and Biodiversity, Department of Bioscience, Aarhus University, Ny Munkegade 114-116, DK-8000 Aarhus C
2. School of GeoSciences, University of Edinburgh, Edinburgh EH9 3FF, UK
3. Senckenberg Gesellschaft für Naturforschung, Biodiversity and Climate Research Centre (BiK-F), Senckenberganlage 25, Frankfurt, Germany
4. Department of Ecology and Evolutionary Biology, University of Colorado, Boulder, Colorado 80309 USA
5. National Ecological Observatory Network, 1685 38th St, Boulder, CO 80301, USA
6. Arctic Research Center, Department of Bioscience, Aarhus University, Ny Munkegade 114-116, DK-8000 Aarhus C
7. Center for Biodiversity Dynamic in a Changing World (BIOCHANGE), Department of Bioscience, Aarhus University, Ny Munkegade 114-116, DK-8000 Aarhus C

8. German Centre for Integrative Biodiversity Research (iDiv) Halle-Jena-Leipzig, Leipzig, Germany
9. Smithsonian Tropical Research Institute, Apartado 0843-03092, Balboa Ancón, Panama
10. European Commission, Joint Research Centre, Directorate D - Sustainable Resources, Bio-Economy Unit, Via Enrico Fermi 2749, 21027, Ispra, Italy
11. Department of Physical Geography and Ecosystem Science, Lund University, Lund S-223 62, Sweden
12. Systems Ecology, Department of Ecological Science, Vrije Universiteit, Amsterdam, The Netherlands
13. Arctic Centre, University of Lapland, FI-96101 Rovaniemi, Finland
14. International Agency for Research in Cancer, Lyon, France
15. Northern Arizona University, Flagstaff, Arizona, USA
16. Bigelow Laboratory for Ocean Sciences, East Boothbay, Maine, USA
17. Department of Geography, University of British Columbia, Vancouver, BC V6T 1Z4, Canada
18. Biology Department, University of Washington, Seattle, USA, 98195-1800
19. Biology Department, Grand Valley State University, 1 Campus Drive, Allendale Michigan USA
20. Swiss Federal Research Institute WSL, Zürcherstrasse 111, 8903 Birmensdorf, Switzerland
21. Max Planck Institute for Biogeochemistry, Jena, Germany
22. WSL Institute for Snow and Avalanche Research SLF, 7260 Davos, Switzerland
23. Department of Evolutionary Biology and Environmental Studies, University of Zurich, Zurich, Switzerland
24. Département de biologie, Université de Sherbrooke, Sherbrooke, Québec, Canada J1K 2R1
25. Institute of Botany and Landscape Ecology, Greifswald University, Greifswald, Germany
26. Department of Chemistry, Life Sciences and Environmental Sustainability, University of Parma, Parco Area delle Scienze 11/A, I-43124 Parma, Italy
27. Department of Biology, Memorial University, St. John's, Newfoundland and Labrador, Canada A1B3X9
28. Département des Sciences de l'environnement et Centre d'études nordiques, Université du Québec à Trois-Rivières, Trois-Rivières, QC, G9A 5H7, Canada
29. Department of Biological and Environmental Sciences, University of Gothenburg, Gothenburg, Sweden
30. Conservation Biology Department, Institute of Environmental Sciences, Leiden University, The Netherlands
31. Department of Evolution, Ecology, and Organismal Biology, University of California Riverside, Riverside, CA.
32. Department of Earth Sciences, University of Gothenburg, P.O. Box 460, SE-405 30 Gothenburg, Sweden
33. Department of Biological and Environmental Sciences, Qatar University, Qatar
34. Department of Forestry, Forest and Wildlife Research Center, Mississippi State University, MS 39762

35. Department of Evolutionary Biology, Ecology and Environmental Sciences, University of Barcelona, Av. Diagonal 643 E-08028 Barcelona
36. Biodiversity Research Institute, University of Barcelona, Av. Diagonal 643 E-08028 Barcelona
37. Department of Ecology and Environmental Science, Umeå University, Sweden
38. Department of Environmental Sciences, Copernicus Institute, Utrecht University, the Netherlands
39. Adam Mickiewicz University, Institute of Geoecology and Geoinformation, B.Krygowskiego 10, 61-680 Poznan, Poland
40. University of Alaska Anchorage, Department of Biological Sciences, 3151 Alumni Loop, Anchorage, Alaska 99508, USA
41. Ecoclimatology, Technische Universität München, Hans-Carl-von-Carlowitz-Platz 2, 85354 Freising
42. The Alaska Department of Fish and Game, 333 Raspberry Road, Anchorage, Alaska 99518
43. Department of Arctic and Marine Biology, Faculty of Biosciences, Fisheries and Economics, UiT- The Arctic University of Norway, NO-9037 Tromsø, Norway
44. Department of Botany and Biodiversity Research, University of Vienna, Rennweg 14, A-1030 Vienna, Austria
45. Center for Permafrost (CENPERM), Department of Geosciences and Natural Resource Management, University of Copenhagen, DK-1350 Copenhagen, Denmark
46. Department of Physiological Diversity, Helmholz Center for Environmental Research - UFZ, Permoserstrasse 15, Leipzig 04103, Germany
47. Department of Ecology, University of Oulu, 90014 University of Oulu, Finland
48. Global Ecology Unit, CREAF-CSIC-UAB, Bellaterra, Catalonia 08193, Spain
49. CREAF, Cerdanyola del Vallès, Catalonia 08193, Spain
50. Department of Biology, Queen's University, Kingston, ON, Canada
51. Biology Department, Swedish Agricultural University (SLU), Uppsala, Sweden
52. Biology Department, Saint Mary's University, Halifax, NS, Canada
53. Plant Ecology and Nature Conservation Group, Wageningen University & Research, Wageningen, The Netherlands
54. British Columbia Public Service, Canada
55. Climate Change Science Institute and Environmental Sciences Division, Oak Ridge National Laboratory, Oak Ridge, TN, USA 37831
56. Institute of Biological and Environmental Sciences, University of Aberdeen, Aberdeen, AB24 3UU
57. Department of Biology, University of Saskatchewan, Saskatoon SK S7N 5E2 Canada
58. Department of Geosciences and Natural Resource Management, University of Copenhagen, Denmark
59. Department of Biology, Vrije Universiteit Brussel (VUB), Belgium
60. Department of Forest Resources Management, Faculty of Forestry, University of British Columbia, Vancouver, BC, Canada
61. School of Environmental Studies, University of Victoria, Victoria, BC, Canada
62. Department of Aquatic Ecology, Eawag: Swiss Federal Institute of Aquatic Science and Technology, Dubendorf, Switzerland

63. NTNU University Museum, Norwegian University of Science and Technology, NO-7491 Trondheim, Norway
64. Department of Biology, University of Copenhagen, Universitetsparken 15, DK-2100 Copenhagen, Denmark
65. Center for Permafrost (CENPERM), University of Copenhagen, Oster Voldgade 10, DK-1350 Copenhagen, Denmark
66. Research Institute for Nature and Forest (INBO), Havenlaan 88, box 73, 1000 Brussels
67. Department of Bioscience, Aarhus University, Frederiksborgvej 399, DK-4000 Roskilde, Denmark
68. Department of Biological Sciences, Florida International University, Miami FL 33199 USA
69. Department of Geobotany, Lomonosov Moscow State University, Moscow 119234, Russia
70. Institute of Northern Engineering, University of Alaska Fairbanks, USA
71. School of Environment, Resources and Sustainability, University of Waterloo, Waterloo, Ontario, Canada N2L 3G1
72. Département de biologie, Centre d'études nordiques and Centre d’étude de la forêt, Université Laval, QC, G1V 0A6, Canada
73. Centre for Integrative Ecology, School of Life and Environmental Sciences, Deakin University, 221 Burwood Highway, Burwood, VIC, Australia 3125
74. Department of Geography, University of Bonn, Meckenheimer Allee 166, D-53115 Bonn, Germany
75. USDA Forest Service International Institute of Tropical Forestry, Río Piedras, Puerto Rico
76. Department of Biological Sciences, University of Alberta, Edmonton, AB, T6G 2E9, Canada
77. Norwegian Institute for Nature Research, PO Box 5685 Sluppen, NO-7485 Trondheim, Norway
78. Faculty of Life and Environmental Sciences, University of Iceland, 101 Reykjavík, Iceland
79. University Centre in Svalbard, N-9171 Longyearbyen, Norway
80. Arctic National Wildlife Refuge, U. S. Fish and Wildlife Service
81. Department of Ecosystem Science & Sustainability, Colorado State University, Campus Delivery 1476, Fort Collins, CO 80523-1476 USA
82. Icelandic Institute of Natural History, Gardabaer, Iceland
83. University of Texas at El Paso, El Paso, Texas, USA
84. Biology and Environmental Sciences, Faculty of Natural Sciences, University of Stirling, Stirling, FK9 4LA, Scotland, UK
85. Institute of Ecology, University of Innsbruck, Innsbruck, Austria
86. Environmental Change Institute, School of Geography and the Environment, South Parks Road, University of Oxford, Oxford OX1 3QY, UK
87. Rocky Mountain Biological Laboratory, PO Box 519, Crested Butte, Colorado, 81224 USA
88. Institute of Environmental Sciences, Leiden University, 2333 CC Leiden, the Netherlands

89. Joint Global Change Research Institute, Pacific Northwest National Laboratory, College Park, MD, USA
90. School of Biosciences & Veterinary Medicine - Plant Diversity and Ecosystems Management unit, Univeristy of Camerino, via Pontoni, 5 - 62032, Italy
91. DiSTA - University of Insubria, via Dunant 3, 21100 Varese, Italy
92. Institute of Arctic Biology, University of Alaska Fairbanks, Fairbanks, AK 99709, USA
93. School of Biological, Earth & Environmental Sciences, Ecology and Evolution Research Centre, UNSW Australia, Sydney, NSW 2052, Australia
94. Jonah Ventures, Manhattan KS 66502, USA
95. Institute for Alpine Environment, Eurac Research, Bolazano, Italy
96. School of Earth and Environmental Sciences, The University of Manchester, UK
97. Instituto Multidisciplinario de Biología Vegetal (IMBIV), CONICET and FCEFyN, Universidad Nacional de Córdoba, Casilla de Correo 495, 5000 Córdoba, Argentina
98. Department of Ecology and Evolutionary Biology, University of Arizona, Tucson, Arizona 85719, USA
99. The Santa Fe Institute, 1399 Hyde Park Road, Santa Fe, New Mexico 87501, USA
100. Department of Organismic and Evolutionary Biology, Harvard University, 26 Oxford Street, Cambridge, MA 02138 USA
101. Área de Biodiversidad y Conservación. Departamento de Biología, Geología, Física y Química Inorgánica. Universidad Rey Juan Carlos, 28933 Móstoles (Madrid), Spain
102. Estonian University of Life Sciences, Kreutzwaldi 1, 51014 Tartu, Estonia
103. Graduate School of Agriculture, Kyoto University, Oiwake, Kitashirakawa, Kyoto, 606-8502 Japan
104. World Agroforestry Centre - Latin America, Av. La Molina 1895, La Molina, Lima, Perú
105. Team Vegetation, Forest and Landscape ecology, Wageningen Environmental Research (Alterra), P.O. Box 47, NL-6700 AA Wageningen, The Netherlands
106. Institute for Water and Wetland Research, Radboud University Nijmegen, 6500 GL Nijmegen, The Netherlands
107. Global Ecology Unit CREAF-CSIC-UAB, Consejo Superior de Investigaciones Cientificas, Bellaterra, Catalonia 08193, Spain
108. Plant Sciences (IBG-2), Forschungszentrum Jülich GmbH, Jülich 52425, Germany
109. Ecology and Conservation Biology, Institute of Plant Sciences, University of Regensburg, D-93040 Regensburg
110. Department of Forest Resources, University of Minnesota, St. Paul, MN 55108 USA
111. Hawkesbury Institute for the Environment, Western Sydney University, Penrith NSW 2751, Australia
112. Department of Biology, Santa Clara University, 500 El Camino Real, Santa Clara, CA, 95053 USA
113. Department of Biology, Algoma University, Sault Ste. Marie, Ontario, Canada
114. Komarov Botanical Institute, Prof. Popov Street 2, St Petersburg 197376, Russia
115. Department of Biology, University of Wisconsin - Eau Claire, Eau Claire, WI 54702, USA

* corresponding author (anne.bjorkman@senckenberg.de)

Summary paragraph

The tundra is warming more rapidly than any other biome on Earth, and the potential ramifications are far-reaching due to global-scale vegetation-climate feedbacks. A better understanding of how environmental factors shape plant structure and function is critical to predicting the consequences of environmental change for ecosystem functioning. Here, we explore the biome-wide relationships between temperature, moisture, and seven key plant functional traits both across space and over three decades of warming at 117 tundra locations. Spatial temperature-trait relationships were generally strong but soil moisture had a marked influence on the strength and direction of these relationships, highlighting the potentially important influence of changes in water availability on future plant trait change. Community height increased with warming across all sites over the past three decades, but other traits lagged far behind predicted rates of change. Our findings highlight the challenge of using space-for-time substitution to predict the functional consequences of future warming and suggest that functions tied closely to plant height will experience the most rapid change. Our results reveal the strength with which environmental factors shape biotic communities at the coldest extremes of the planet and will enable improved projections of tundra functional change with climate warming.

Main text

Rapid climate warming in Arctic and alpine regions is driving changes in the structure and composition of tundra ecosystems[1,2], with potentially global consequences. Up to 50% of the world's belowground carbon stocks are contained in permafrost soils[3], and tundra regions are expected to contribute the majority of warming-induced soil carbon loss over the next century[4]. Plant traits strongly impact carbon cycling and energy balance, which can in turn influence regional and global climates[5-7]. Traits related to the resource economics spectrum[8], such as specific leaf area, leaf nitrogen content, and leaf dry matter content, affect primary productivity, litter decomposability, soil carbon storage, and nutrient cycling[5,6,9,10], while size-related traits such as leaf area and plant height influence aboveground carbon storage, albedo, and hydrology[11-13] (Extended Data Table 1). Quantifying the link between the environment and plant functional traits is therefore critical to understanding the consequences of climate change, but such studies rarely extend into the tundra[14-16]. Thus, the full extent of the relationship between climate and plant traits in the planet's coldest ecosystems has never been assessed, and the consequences of climate warming for tundra functional change are largely unknown.

Here, we quantify for the first time the biome-wide relationships between temperature, soil moisture, and key traits that represent the foundation of plant form and function[17], using the largest dataset of tundra plant traits ever assembled (56,048 measured trait observations; Fig. 1a and Extended Data Fig. 1a, Table S1). We examine five continuously distributed traits related to plant size (adult plant height and leaf area) and to resource economy (specific leaf area (SLA), leaf nitrogen content (leaf N), and leaf dry matter content (LDMC)), as well as two categorical traits related to community-level structure (woodiness) and leaf phenology/lifespan (evergreenness). Intraspecific trait variability is thought to be especially important where diversity is low or where species have wide geographic ranges[18], as in the tundra. Thus, we analyze two underlying components of biogeographic patterns in the five continuous traits: intraspecific variability (phenotypic plasticity or genetic differences among populations) and community-level variability (species turnover or shifts in species' abundances over space). We ask: 1) How do plant traits vary with temperature and soil moisture across the tundra biome? 2) What is the relative influence of intraspecific trait variability (ITV) versus community-level trait variation (estimated as community-weighted trait means, CWM) for spatial temperature-trait relationships? 3) Are spatial temperature-trait relationships explained by among-site differences in species abundance or species turnover (presence-absence)?

A major impetus for quantifying spatial temperature-trait relationships is to provide an empirical basis for predicting the potential consequences of future warming[19-21]. Thus, we also estimate realized rates of community-level trait change over time using nearly three decades of vegetation survey data at 117 tundra sites (Fig. 1a, Table S2). Focusing on interspecific trait variation, we ask: 4) How do changes in community traits over three decades of ambient warming compare to predictions from spatial temperature-trait relationships? We expect greater temporal trait change when spatial temperature-trait relationships are a) strong, b) unlimited by moisture availability, and c) due primarily to abundance shifts instead of species turnover, given that species turnover over time depends on immigration and is likely to be slow[22]. Finally, because total realized trait change in continuous traits is comprised of both community-level variation and intraspecific trait variation (ITV), we estimated the *potential* contribution of ITV to overall trait change (CWM+ITV) using the modeled intraspecific temperature-trait relationships described above (see Methods and Extended Data Fig. 1b). For all analyses, we used a generalizable Bayesian modeling approach, which allowed us to account for the hierarchical spatial, temporal and taxonomic structure of the data as well as multiple sources of uncertainty.

Environment-trait relationships across the tundra biome

We found strong spatial associations between temperature and community height, SLA, and LDMC (Fig. 2a, Extended Data Fig. 2, Table S3) across the 117 survey sites. Both height and SLA increased with summer temperature, but the temperature-trait relationship for SLA was much stronger at wet than at dry sites. LDMC was negatively related to temperature, and more strongly so at wet than at dry sites. Community woodiness decreased with temperature, but the ratio of evergreen to deciduous woody species increased with temperature, particularly in dry sites (Extended Data Fig. 3). These spatial temperature-trait relationships suggest that long-term climate warming should cause pronounced shifts toward communities of taller plants with more resource-acquisitive leaves (high SLA and low LDMC), particularly where soil moisture is high.

Our results reveal a substantial moderating influence of soil moisture on community traits across spatial temperature gradients[2,23]. Both leaf area and leaf N decreased with warmer temperatures in dry sites but increased with warmer temperatures in wet sites (Fig. 2a, Table S4). Soil moisture was important in explaining spatial variation in all seven traits investigated here, even when temperature alone was not (e.g., leaf area; Fig. 2a and Extended Data Figure 2), potentially reflecting physiological constraints related to heat exchange or frost tolerance when water availability is low[24]. Thus, future warming-driven changes in traits and associated ecosystem functions (e.g. decomposability) will likely depend on current soil moisture conditions at a site[23]. Furthermore, future changes in water availability (e.g., via changes in precipitation, snow melt timing, permafrost, and hydrology[25]) could cause substantial shifts in these traits and their associated functions irrespective of warming.

We found consistent intraspecific temperature-trait relationships for all five continuous traits (Fig. 2b, Table S5). Intraspecific plant height and leaf area showed strong positive relationships with summer temperature (i.e., individuals were taller and had larger leaves in warmer locations) while intraspecific LDMC, leaf N and SLA were related to winter but not summer temperature (Extended Data Fig. 2). The differing responses of intraspecific trait variation to summer versus winter temperatures may indicate that size-related traits better reflect summer growth potential while resource economics traits reflect tolerance of cold-stress. These results, although correlative, suggest that trait variation expressed at the individual or population level is related to the growing environment and that warming will likely lead to substantial intraspecific trait change in many traits. Thus, the potential for trait change over time is underestimated by using species-level trait means alone. Future work is needed to disentangle the role of plasticity and genetic differentiation in explaining the observed intraspecific temperature-trait relationships[26], as this will also influence the rate of future trait change[27]. Trait measurements collected over time and under novel (experimental) conditions, as yet unavailable, would enable more accurate predictions of future intraspecific trait change.

Partitioning the underlying causes of community temperature-trait relationships revealed that species turnover explained most of the variation in traits across space (Fig. 2c), suggesting that dispersal and immigration processes will primarily govern the rate of ecosystem responses to warming. Shifts in species' abundances and intraspecific trait variation accounted for a relatively small part of the overall temperature-trait relationship across space (Fig 2c). Furthermore, the local trait pool in the coldest tundra sites (mean summer temperature < 3 °C) is constrained relative to the tundra as a whole for many traits (Extended Data Fig. 4). Together, these results indicate that the magnitude of warming-induced community trait shifts will be limited without the arrival of novel species from warmer environments.

Community trait change over time

Plant height was the only trait for which the community weighted mean changed over the 27 years of monitoring; it increased rapidly at nearly every survey site (Fig. 3 a&b, Extended Data Fig. 3, Table S6). Inter-annual variation in community height was sensitive to summer temperature (Fig. 3c, Extended Data Fig. 2, Table S7), implying that increases in community height are responding to warming. However, neither the total rate of temperature change nor soil moisture predicted the total rate of CWM change in any trait (Extended Data Fig. 5, Table S8). Incorporating potential intraspecific trait variation (ITV) doubled the average estimate of plant height change over time (Fig. 3a and 4a, dashed lines). Because spatial patterns in ITV can be due to both phenotypic plasticity and genetic differences among populations, this is likely a maximum estimate of the ITV contribution, for example if intraspecific temperature-trait relationships are due entirely to phenotypic plasticity. The increase in community height observed here is consistent with previous findings of increasing vegetation height in response to experimental warming at a subset of these sites[28] and with studies showing increased shrub growth over time[11].

Increasing community height over time was due largely to species turnover (rather than shifts in abundance of the resident species; Fig 3b) and was driven by the immigration of taller species rather than the loss of shorter ones (Extended Data Fig. 6, Table S9). This turnover could reflect the movement of tall species upward in latitude and elevation or from local species pools in nearby warmer microclimates. The magnitude of temporal change was comparable to that predicted from the spatial temperature-trait relationship (Fig. 4a, solid lines), indicating that temporal change in plant height is not currently limited by immigration rates. The importance of immigration in explaining community height change is surprising given the relatively short study duration and long lifespan of tundra plants, but is nonetheless consistent with a previous finding of shifts towards warm-associated species in tundra plant communities[20,29]. If the observed rate of trait change continues (e.g., if immigration were unlimited), community height (excluding potential change due to ITV) could increase by 20-60% by the end of the century, depending on carbon emission, warming and water availability scenarios (Extended Data Fig. 7).

Consequences & Implications

Recent (observed) and future (predicted) changes in plant traits, particularly height, are likely to have important implications for ecosystem functions and feedbacks involving soil temperature[30,31], decomposition[5,10], and carbon cycling[32], as the potential for soil carbon loss is particularly great in high-latitude regions[4]. For example, increasing plant height could offset warming-driven carbon loss via increased carbon storage due to woody litter production[5] or via reduced decomposition due to lower summer soil temperatures caused by shading[3,30,32] (negative feedbacks). Positive feedbacks are also possible if branches or leaves above the snowpack reduce albedo[11,12] or increase snow accumulation, leading to warmer winter soil temperatures and increased decomposition rates[3,11]. The balance of these feedbacks and thus the net impact of trait change on carbon cycling may depend on the interaction between warming and changes in snow distribution[33] and water availability[34], which remain major unknowns in the tundra biome.

The lack of an observed temporal trend in SLA and LDMC despite strong temperature-trait relationships over space highlights the limitations of using space-for-time substitution for predicting short-term ecological change. This disconnect could reflect the influence of unmeasured changes in water availability, e.g. due to local-scale variation in the timing of snowmelt or hydrology, that counter or swamp the effect of static soil moisture estimates. For example, we would not expect substantial changes in traits demonstrating a spatial temperature x moisture interaction (LDMC, leaf area, leaf N, and SLA), even in wet sites, if warming also leads to drier soils. Perhaps tellingly, plant height was the only continuous trait for which a temperature x moisture interaction was not important, and was predicted to increase across all areas of the tundra regardless of recent soil moisture trends (Fig. 4c&d). Spatial-temporal disconnects could also reflect dispersal limitation of potential immigrants (e.g., with low LDMC and high SLA), or establishment failure due to novel biotic (e.g., herbivore[35]) or abiotic (e.g., photoperiod[36]) conditions other than temperature to which immigrants are maladapted[22,36]. Furthermore, community responses to climate warming could be constrained by soil properties (e.g., organic matter, mineralization) that themselves respond slowly to warming[20].

The patterns in functional traits described here reveal the extent to which environmental factors shape biotic communities in the tundra. Strong temperature- and moisture-related spatial gradients in traits related to competitive ability (e.g., height) and resource capture and retention (e.g., leaf nitrogen, SLA) reflect tradeoffs in plant ecological strategy[9,37] from benign (warm, wet) to extreme (cold, dry) conditions. Community-level trait syndromes, as reflected in ordination axes, are also strongly related to both temperature and moisture, suggesting that environmental drivers structure not only individual traits but also trait combinations and thus lead to a limited number of successful functional strategies in some environments (e.g., woody, low-SLA and low-leaf N communities in warm, dry sites; Extended Data Fig. 8). Thus, warming may lead to a community-level shift toward more acquisitive plant strategies[37] in wet tundra sites, but toward more conservative strategies in drier sites as moisture becomes more limiting.

Earth system models are increasingly moving to incorporate trait-environment relationships, as this can substantially improve estimates of ecosystem change[38-40]. Our results inform these projections of future tundra functional change[38] by explicitly quantifying the link between temperature, moisture, and key functional traits across the biome. In particular, our study highlights the importance of accounting for future changes in water availability, as this will likely influence both the magnitude and direction of change for many traits. In addition, we demonstrate that spatial trait-environment relationships are driven largely by species turnover, suggesting that modeling efforts must account for rates of species immigration when predicting the speed of future functional shifts. The failure of many traits (e.g. specific leaf area) to match expected rates of change suggests that space-for-time substitution alone may inaccurately represent near-term ecosystem change. Nevertheless, the ubiquitous increase in community plant height reveals that functional change is already occurring in tundra ecosystems.

References

1. Post, E. *et al.* Ecological dynamics across the Arctic associated with recent climate change. *Science* **325,** 1355–1358 (2009).
2. Elmendorf, S. C. *et al.* Plot-scale evidence of tundra vegetation change and links to recent summer warming. *Nature Climate Change* **2,** 453–457 (2012).
3. Sistla, S. A. *et al.* Long-term warming restructures Arctic tundra without changing net soil carbon storage. *Nature* **497,** 615–618 (2013).
4. Crowther, T. W. *et al.* Quantifying global soil carbon losses in response to warming. *Nature* **540,** 104–108 (2016).
5. Cornelissen, J. H. C. *et al.* Global negative vegetation feedback to climate warming responses of leaf litter decomposition rates in cold biomes. *Ecology Letters* **10,** 619–627 (2007).
6. Lavorel, S. & Garnier, E. Predicting changes in community composition and ecosystem functioning from plant traits: revisiting the Holy Grail. *Functional Ecology* **16,** 545–556 (2002).
7. Pearson, R. G. *et al.* Shifts in Arctic vegetation and associated feedbacks under climate change. *Nature Climate Change* **3,** 673–677 (2013).
8. Wright, I. J. *et al.* The worldwide leaf economics spectrum. *Nature* **428,** 821–827 (2004).
9. Díaz, S. *et al.* The plant traits that drive ecosystems: Evidence from three continents. *Journal of Vegetation Science* **15,** 295–304 (2004).
10. Cornwell, W. K. *et al.* Plant species traits are the predominant control on litter decomposition rates within biomes worldwide. *Ecology Letters* **11,** 1065–1071 (2008).
11. Myers-Smith, I. H. *et al.* Shrub expansion in tundra ecosystems: dynamics, impacts and research priorities. *Environ. Res. Lett.* **6,** 045509 (2011).
12. Sturm, M. & Douglas, T. Changing snow and shrub conditions affect albedo with global implications. *J. Geophys. Res.* **110,** G01004 (2005).
13. Callaghan, T. V. *et al.* Effects on the Function of Arctic Ecosystems in the Short- and Long-Term Perspectives. *AMBIO* **33,** 448–458 (2004).
14. Moles, A. T. *et al.* Global patterns in plant height. *Journal of Ecology* **97,** 923–932 (2009).
15. Moles, A. T. *et al.* Global patterns in seed size. *Global Ecology and Biogeography* **16,** 109–116 (2007).
16. Reich, P. B. & Oleksyn, J. Global patterns of plant leaf N and P in relation to temperature and latitude. *Proc. Natl. Acad. Sci. U.S.A.* **101,** 11001–11006 (2004).

17. Díaz, S. *et al.* The global spectrum of plant form and function. *Nature* **529,** 167–171 (2016).
18. Siefert, A. *et al.* A global meta-analysis of the relative extent of intraspecific trait variation in plant communities. *Ecology Letters* **18,** 1406–1419 (2015).
19. McMahon, S. M. *et al.* Improving assessment and modelling of climate change impacts on global terrestrial biodiversity. *Trends Ecol. Evol.* **26,** 249–259 (2011).
20. Elmendorf, S. C. *et al.* Experiment, monitoring, and gradient methods used to infer climate change effects on plant communities yield consistent patterns. *Proc. Natl. Acad. Sci. U.S.A.* **112,** 448–452 (2015).
21. De Frenne, P. *et al.* Latitudinal gradients as natural laboratories to infer species' responses to temperature. *Journal of Ecology* **101,** 784–795 (2013).
22. Sandel, B. *et al.* Contrasting trait responses in plant communities to experimental and geographic variation in precipitation. *New Phytologist* **188,** 565–575 (2010).
23. Ackerman, D., Griffin, D., Hobbie, S. E. & Finlay, J. C. Arctic shrub growth trajectories differ across soil moisture levels. **23,** 4294–4302 (2017).
24. Wright, I. J. *et al.* Global climatic drivers of leaf size. *Science* **357,** 917–921 (2017).
25. Wrona, F. J. *et al.* Transitions in Arctic ecosystems: Ecological implications of a changing hydrological regime. *Journal of Geophysical Research: Biogeosciences* **121,** 650–674 (2016).
26. Read, Q. D., Moorhead, L. C., Swenson, N. G., Bailey, J. K. & Sanders, N. J. Convergent effects of elevation on functional leaf traits within and among species. *Functional Ecology* **28,** (2014).
27. Albert, C. H., Grassein, F., Schurr, F. M., Vieilledent, G. & Violle, C. When and how should intraspecific variability be considered in trait-based plant ecology? *Perspectives in Plant Ecology, Evolution and Systematics* **13,** 217–225 (2011).
28. Elmendorf, S. C. *et al.* Global assessment of experimental climate warming on tundra vegetation: heterogeneity over space and time. *Ecology Letters* **15,** 164–175 (2012).
29. Gottfried, M. *et al.* Continent-wide response of mountain vegetation to climate change. *Nature Climate Change* **2,** 111–115 (2012).
30. Blok, D. *et al.* Shrub expansion may reduce summer permafrost thaw in Siberian tundra. *Global Change Biology* **16,** 1296–1305 (2010).
31. Blok, D., Elberling, B. & Michelsen, A. Initial stages of tundra shrub litter decomposition may be accelerated by deeper winter snow but slowed down by spring warming. *Ecosystems* **19,** 155–169 (2016).

32. Cahoon, S. M. P., Sullivan, P. F., Shaver, G. R., Welker, J. M. & Post, E. Interactions among shrub cover and the soil microclimate may determine future Arctic carbon budgets. *Ecology Letters* **15,** 1415–1422 (2012).
33. Lawrence, D. M. & Swenson, S. C. Permafrost response to increasing Arctic shrub abundance depends on the relative influence of shrubs on local soil cooling versus large-scale climate warming. *Environ. Res. Lett.* **6,** 045504 (2011).
34. Christiansen, C. T. *et al.* Enhanced summer warming reduces fungal decomposer diversity and litter mass loss more strongly in dry than in wet tundra. *Global Change Biology* **23,** 406–420 (2017).
35. Kaarlejärvi, E., Eskelinen, A. & Olofsson, J. Herbivores rescue diversity in warming tundra by modulating trait-dependent species losses and gains. *Nat Comms* **8,** 1–8 (2017).
36. Bjorkman, A. D., Vellend, M., Frei, E. R. & Henry, G. H. R. Climate adaptation is not enough: warming does not facilitate success of southern tundra plant populations in the high Arctic. *Global Change Biology* **23,** 1540–1551 (2017).
37. Reich, P. B. The world-wide 'fast–slow' plant economics spectrum: a traits manifesto. *Journal of Ecology* **102,** 275–301 (2014).
38. Wullschleger, S. D. *et al.* Plant functional types in Earth system models: past experiences and future directions for application of dynamic vegetation models in high-latitude ecosystems. *Annals of Botany* **114,** 1–16 (2014).
39. Butler, E. E. *et al.* Mapping local and global variability in plant trait distributions. *Proc. Natl. Acad. Sci. U.S.A.* **114,** E10937–E10946 (2017).
40. Reich, P. B., Rich, R. L., Lu, X., Wang, Y.-P. & Oleksyn, J. Biogeographic variation in evergreen conifer needle longevity and impacts on boreal forest carbon cycle projections. *Proceedings of the National Academy of Sciences* **111,** 13703–13708 (2014).

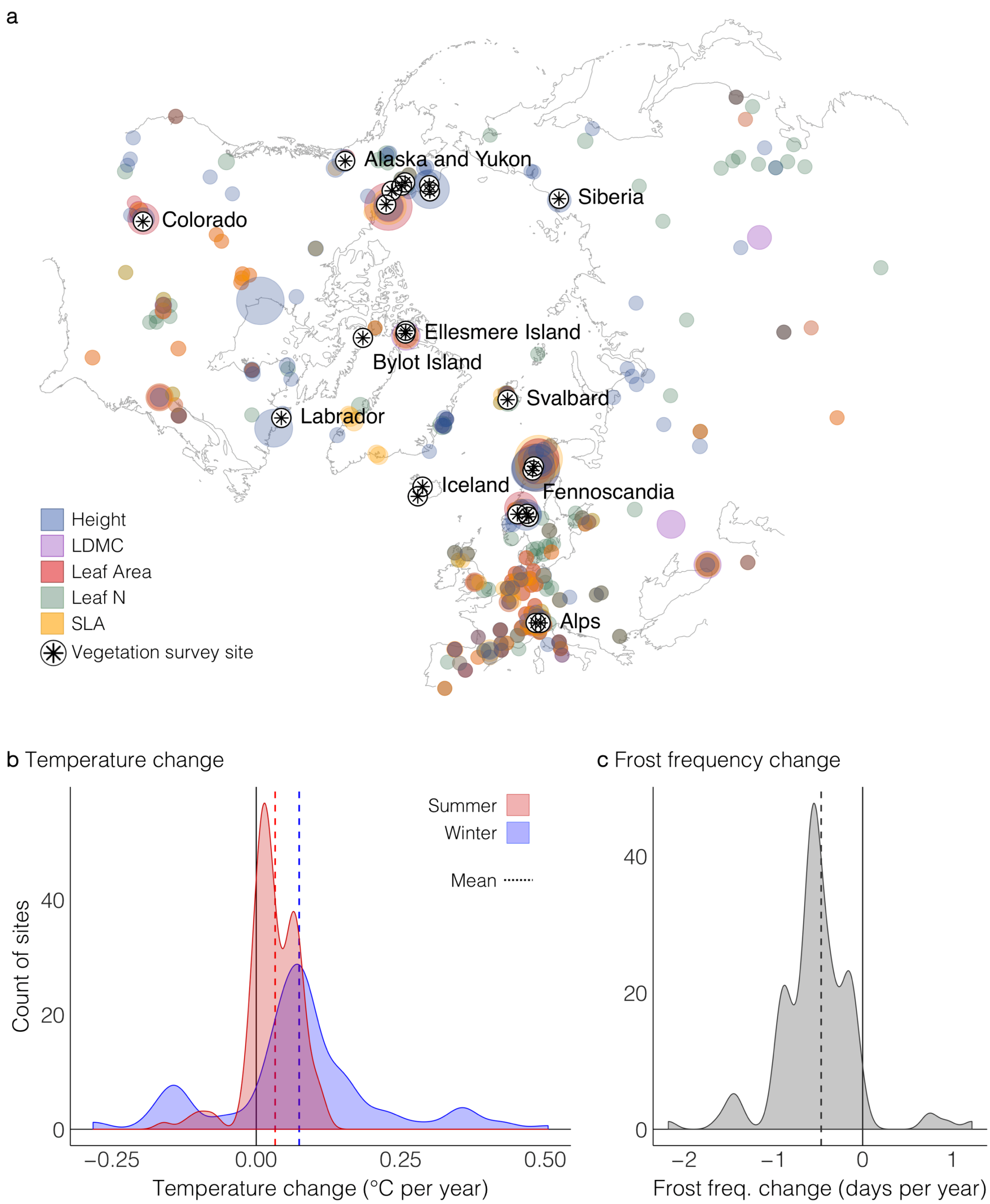

Figure 1. Geographic distribution of trait and vegetation survey data and climatic change over the study period. a. Map of all 56,048 tundra trait records and 117 vegetation survey sites. **b-c.** Climatic change across the period of monitoring at the 117 vegetation survey sites, represented as mean winter (coldest quarter) and summer (warmest quarter) temperature (**b**) and frost day frequency (**c**). The size of the colored points on the map indicates the relative quantity of trait measurements (larger circles = more measurements of that trait at a given location) and the color indicates which trait was measured. The black

stars indicate the vegetation survey sites used in the community trait analyses (most stars represent multiple sites). Trait data were included for all species that occur in at least one tundra vegetation survey site; thus, while not all species are unique to the tundra, all do occur in the tundra. Temperature change and frost frequency change were estimated for the interval over which sampling was conducted at each site plus the preceding four years in order to best reflect the time window over which tundra plant communities respond to temperature change[20,29].

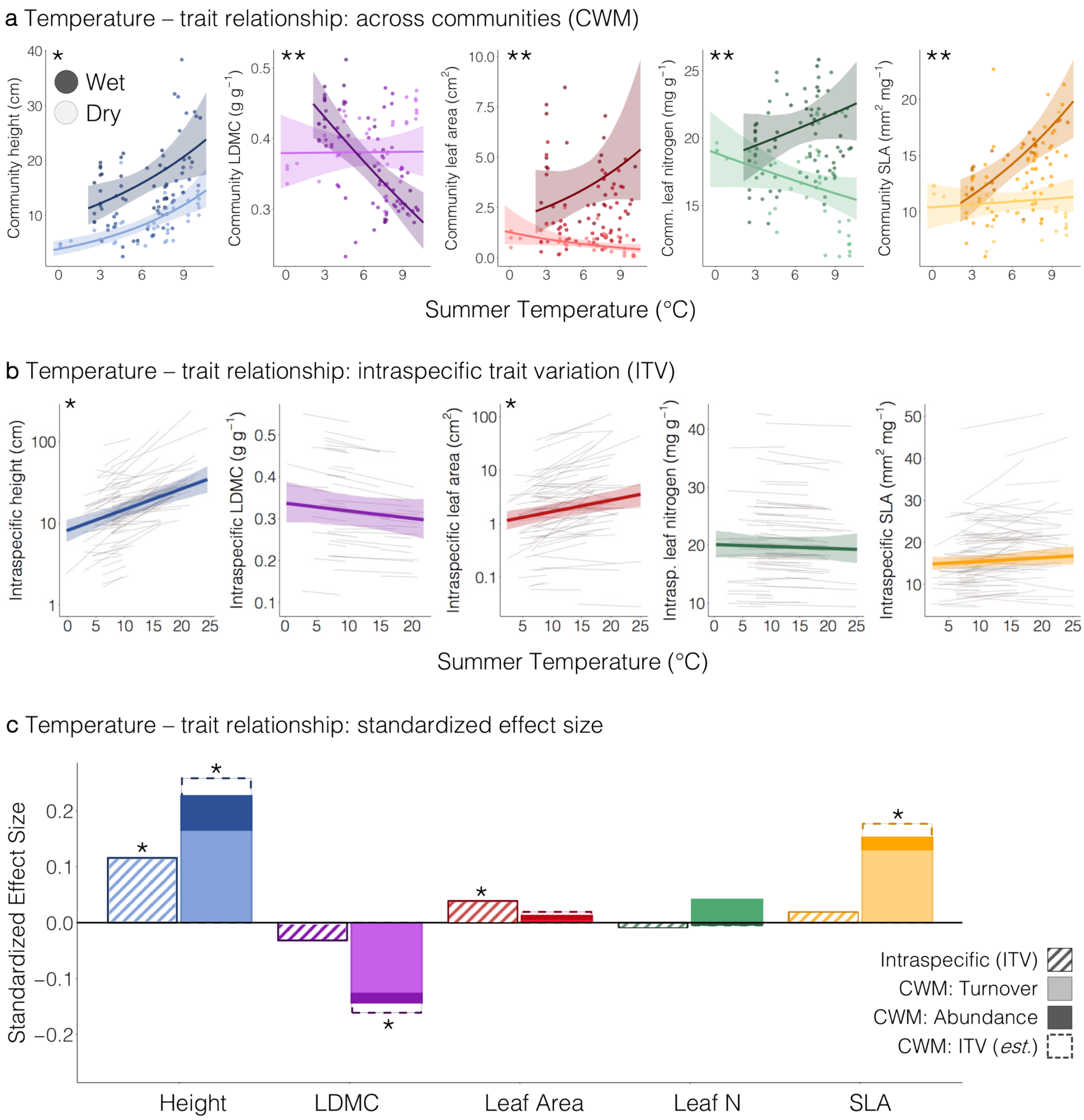

Figure 2. Strong spatial relationships in traits across temperature and soil moisture gradients are primarily explained by species turnover. a, Community-level (CWM) variation in functional traits across space (N = 1520 plots within 117 sites within 72 regions)

as related to mean summer (warmest quarter) temperature and soil moisture, and **b,** intraspecific variation (ITV) across space as related to summer temperature (note the log scale for height and leaf area). **c,** Standardized effect sizes were estimated for all temperature-trait relationships both across communities (CWM; solid bars) and within species (ITV; striped bars). Effect sizes for CWM temperature-trait relationships were further partitioned into the proportion of the effect driven solely by species turnover (light bars) and abundance shifts (dark bars) over space. Dashed lines indicate the estimated total temperature-trait relationship over space if intraspecific trait variability is also accounted for (CWM: ITV). The contribution of ITV is estimated from the spatial temperature-trait relationships modeled in (**b**). Soil moisture in (**a**) was modeled as continuous but is shown predicted only at low and high values to improve visualization. Transparent ribbons in (**a**) and (**b**) indicate 95% credible intervals for model mean predictions. Grey lines in (**b**) represent intraspecific temperature-trait relationships for each species (height: N = 80 species, LDMC: N = 43, leaf area: N = 85, leaf N: N = 85, SLA: N = 108; N of observations per trait shown in Table S1). In all panels, asterisks indicate that the 95% credible interval on the slope of the temperature-trait relationship did not overlap zero. In panel (**a**), two asterisks indicate that the temperature x soil moisture interaction term did not overlap zero. Winter temperature – trait relationships are shown in Extended Data Fig. 2. Community woodiness and evergreenness are shown in Extended Data Fig. 3.

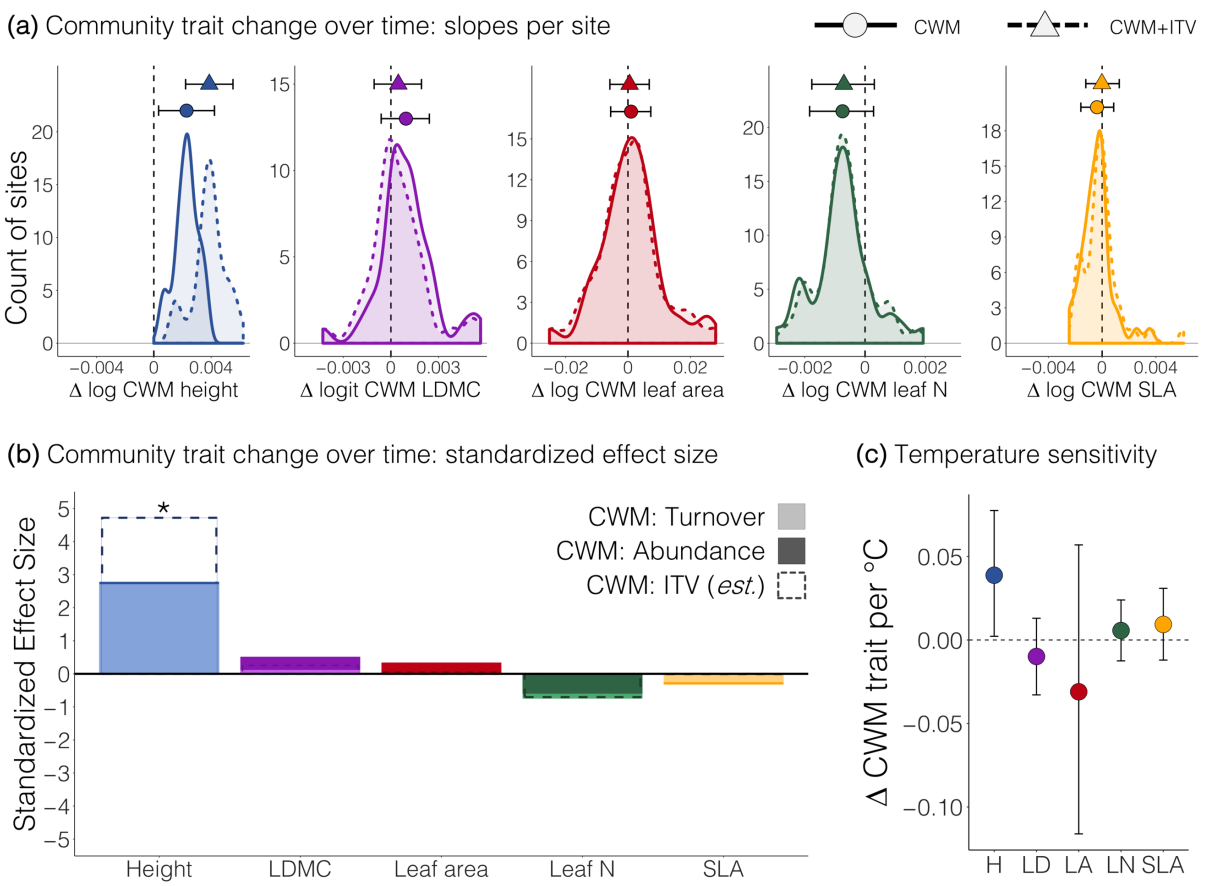

Figure 3. A tundra-wide increase in community height over time is related to warming. **a,** Observed community trait change per year (transformed units). Solid lines indicate the distribution of community-weighted mean (CWM) model slopes (trait change per site) while dashed lines indicate the community-weighted mean plus potential intraspecific trait variation modelled from spatial temperature-trait relationships (CWM+ITV). Circles (CWM), triangles (CWM+ITV) and error bars indicate the mean and 95% credible interval for the overall rate of trait change across all sites (N = 4575 plot-years within 117 sites within 38 regions). The vertical black dashed line indicates 0 (no change over time). **b,** Standardized effect sizes for CWM change over time were further partitioned into the proportion of the effect driven solely by species turnover (light bars) or shifts in abundance of resident species (dark bars) over time. Dashed lines indicate the estimated total trait change over time if predicted intraspecific trait variability is also included (CWM+ITV). Stars indicate that the 95% CI on the mean hyperparameter for CWM trait change over time did not overlap zero. **c,** Temperature sensitivity of each trait as related to summer temperature (i.e., correspondence between interannual variation in CWM trait values and interannual variation in temperature). Temperatures associated with each survey year were estimated as five-year means (temperature of the survey year and four preceding years) because this interval has been shown to be most relevant to vegetation change in tundra[20] and alpine[29] plant communities.

Circles represent the mean temperature sensitivity across all 117 sites, error bars are 95% credible intervals on the mean. Changes in community woodiness and evergreenness are shown in Extended Data Fig. 3.

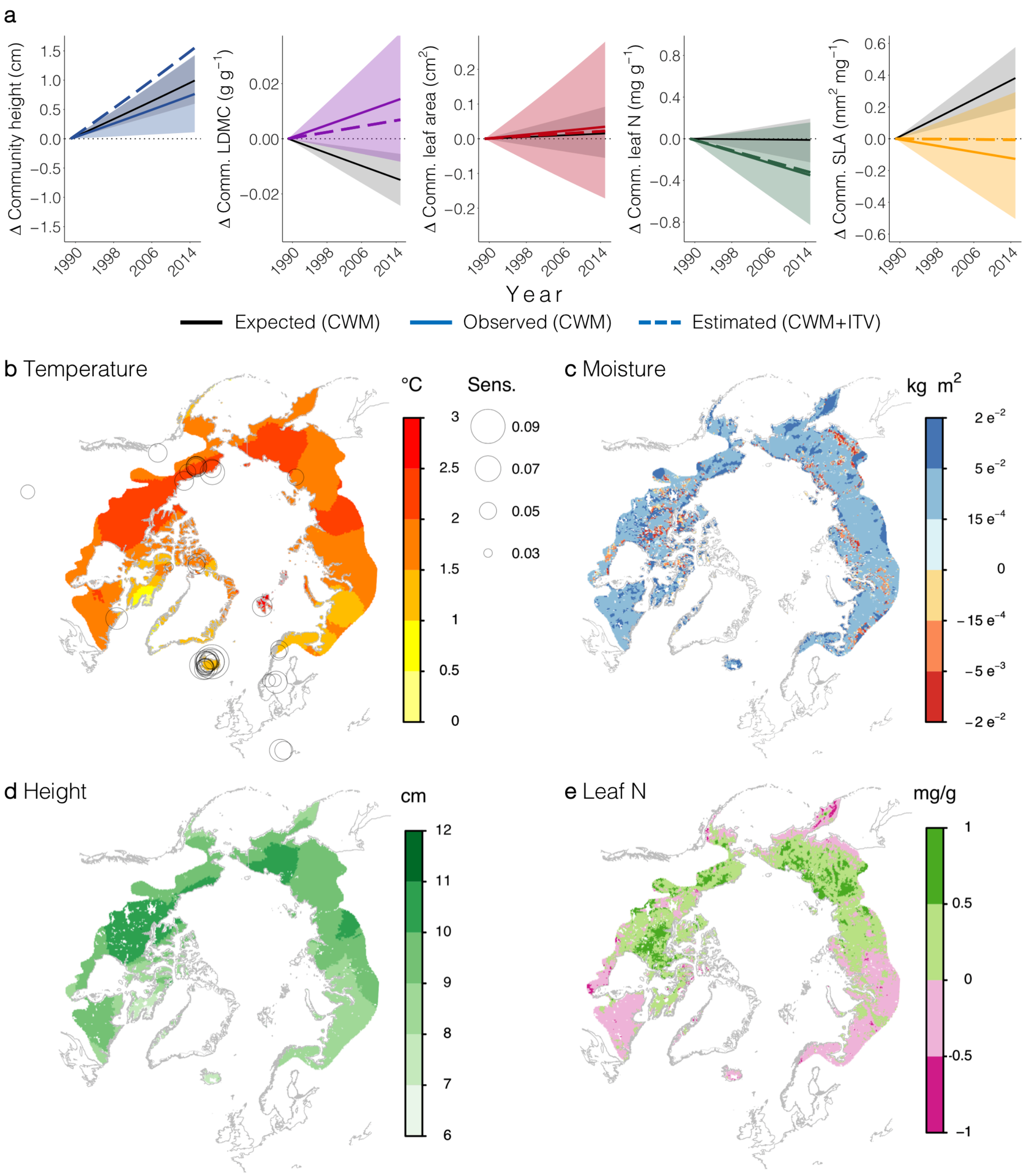

Figure 4. Community height increases in line with space-for-time predictions but other traits lag. a, Observed community (CWM) trait change over time (colored lines) across all 117 sites vs. expected CWM change over the duration of vegetation monitoring (1989-2015) based on the spatial temperature-trait (CWM) relationship and the average rate of recent summer warming across all sites (solid black lines). Colored dashed lines indicate

the estimated total change over time if predicted intraspecific trait variability is also included (CWM+ITV). Values on the y-axis represent the magnitude of change relative to 0 (i.e., trait anomaly), with 0 representing the trait value at t_0. **b-c,** Total recent temperature change (**b**) and soil moisture change (**c**) across the Arctic tundra (1979-2016). Temperature change estimates are derived from CRU gridded temperature data, soil moisture change estimates are derived from downscaled ERA-Interim soil moisture data. Circles in (**b**) represent the sensitivity (cm per °C) of CWM plant height to summer temperature at each site (see Fig. 3c). Areas of high temperature sensitivity are expected to experience the greatest increases in height with warming. **d-e,** Spatial trait-temperature-moisture relationships (Fig. 2a) were used to predict total changes in height (**d**) and leaf N (**e**) over the entire 1979-2016 period based on concurrent changes in temperature and soil moisture. Note that (**d**) and (**e**) reflect the magnitude of *expected* change between 1979 and 2016, not observed trait change. See methods for details of temperature change and soil moisture change estimates. The outline of Arctic areas is based on the Circumpolar Arctic Vegetation Map (http://www.geobotany.uaf.edu/cavm).

Acknowledgements

This paper is an outcome of the sTundra working group supported by sDiv, the Synthesis Centre of the German Centre for Integrative Biodiversity Research (iDiv) Halle-Jena-Leipzig (DFG FZT 118). ADB was supported by an iDiv postdoctoral fellowship and The Danish Council for Independent Research - Natural Sciences (DFF 4181-00565 to SN). ADB, IHM-S, HJDT and SA-B were funded by the UK Natural Environment Research Council (ShrubTundra Project NE/M016323/1 to IHM-S) and SN by the Villum Foundation's Young Investigator Programme (VKR023456). NR was supported by the DFG-Forschungszentrum 'German Centre for Integrative Biodiversity Research (iDiv) Halle-Jena-Leipzig' and Deutsche Forschungsgemeinschaft DFG (RU 1536/3-1). AB was supported by EU-F7P INTERACT (262693) and MOBILITY PLUS (1072/MOB/2013/0). ABO and SSN were supported by the Danish Council for Independent Research - Natural Sciences (DFF 4181-00565 to SN) and the Villum Foundation (VKR023456 to SN). SSN was additionally supported by the Carlsberg Foundation (2013-01-0825). JMA was supported by the Carl Tryggers stiftelse för vetenskaplig forskning, AH by the Research Council of Norway (244557/E50), BE by the Danish National Research Foundation (CENPERM DNRF100), BM by the Soil Conservation Service of Iceland, and ERF by the Swiss National Science Foundation (#155554). BCF was supported by the Academy of Finland (256991) and JPI Climate (291581). BJE was supported by an NSF ATB, CAREER, and Macrosystems award. CMI was supported by the Office of Biological and Environmental Research in the U.S. Department of Energy's Office of Science as part of the Next-Generation Ecosystem Experiments in the Arctic (NGEE Arctic) project. DB was supported by The Swedish Research Council (2015-00465) and Marie Skłodowska Curie Actions co-funding (INCA 600398). EW was supported by the National Science Foundation (DEB-0415383), UWEC - ORSP, and UWEC - BCDT. GS-S and MIG were supported by the University of Zurich Research Priority Program on Global Change and Biodiversity. HA was supported by NSF PLR (1623764, 1304040). ISJ was supported by the Icelandic Research Fund (70255021) and the University of Iceland Research Fund. JDMS was supported by the Research Council of Norway (262064). JSP was supported by the U. S. Fish and Wildlife Service. JCO was supported by Klimaat voor ruimte, Dutch national research program Climate Change and Spatial Planning. J. Johnstone, PG, GHRH, NB-L, KAH, LSC and TZ were supported by the Natural Sciences and Engineering Research Council of Canada (NSERC). GHRH, NB-L, LSC and LH were supported by ArcticNet. GHRH, NB-L and LSC were supported by the Northern Scientific Training Program. GHRH and NB-L were additionally supported by the Polar Continental Shelf Program. NB-L was additionally supported by the Fonds de recherche du Quebec: Nature et technologies and the Centre d'études Nordiques. JP was supported by the European Research Council Synergy grant SyG-2013-610028 IMBALANCE-P. AAR, OG and JMN were supported by the Spanish OAPN (project 534S/2012) and European INTERACT project (262693 Transnational Access). KDT was supported by NSF ANS-1418123. LS and PAW were supported by the UK Natural Environment Research Council Arctic Terrestrial Ecology Special Topic Programme and Arctic Programme (NE/K000284/1 to PAW). PAW was additionally supported by the European Union 4th Environment and Climate Framework Programme (Project Number ENV4-CT970586). MW was supported by DFG RTG 2010. RDH was supported by the US National Science Foundation. SJG was supported by NASA NNX15AU03A. HJDT was funded by a NERC doctoral training partnership grant (NE/L002558/1). VGO was supported by the Russian Science Foundation (#14-50-00029). LB was supported by NSF ANS (1661723) and SJG by NASA ABoVE (NNX17AE44G). BB-L was supported as part of the Energy Exascale Earth System Model (E3SM) project, funded by the U.S. Department of Energy, Office of Science, Office of Biological and Environmental Research. AE was supported by the Academy of Finland (projects 253385 and 297191). The study has been supported by the TRY initiative on plant traits (http://www.try-db.org), which is hosted at the Max Planck Institute for Biogeochemistry, Jena, Germany and is currently supported by DIVERSITAS/Future Earth and the German Centre for Integrative Biodiversity Research (iDiv) Halle-Jena-Leipzig. ADB and SCE thank the US National Science Foundation for support to receive training in Bayesian methods (grant # 1145200 to N. Thompson Hobbs). The authors thank Helge Bruelheide and Julian Ramirez-Villegas for helpful input at earlier stages of this project. We acknowledge the contributions of Steven Mamet, Mélanie Jean, Kirsten Allen, Nathan Young, Jenny Lowe, Olof Eriksson, and many others to trait and community composition data collection, and thank the governments, parks, field stations and local and indigenous people for the opportunity to conduct research on their land.

Author contributions

ADB, IHM-S and SCE conceived the study, with input from the sTundra working group (SN, NR, PSAB, AB-O, DB, JHCC, WC, BCF, DG, SJG, KG, GHRH, RDH, JK, JSP, JHRL, CR, GS-S, HJDT, MV, MW, and SW). ADB performed the analyses, with input from IHM-S, NR, SCE, and SN. DNK made the maps of temperature, moisture, and trait change. ADB wrote the manuscript, with input from IHM-S, SCE, SN, NR, and contributions from all authors. ADB compiled the Tundra Trait Team database, with assistance from IHM-S, HJDT and SA-B. Authorship order was determined as follows: 1) core authors, 2) sTundra participants (alphabetical) and other major contributors, 3) authors contributing both trait (Tundra Trait Team) and community composition (ITEX, etc.) data (alphabetical), 4) Tundra Trait Team contributors (alphabetical), 5) community composition data only contributors (alphabetical), and 6) TRY trait data contributors (alphabetical).

Author Information

Reprints and permissions information is available at www.nature.com/reprints.

The authors declare no competing financial interests.

Correspondence and requests for materials should be addressed to anne.bjorkman@senckenberg.de.

METHODS

Below we describe the data, workflow (Extended Data Fig. 1b) and detailed methods used to conduct all analyses.

COMMUNITY COMPOSITION DATA

Community composition data used for calculating community-weighted trait means were compiled from a previous synthesis of tundra vegetation resurveys[2] (including many International Tundra Experiment (ITEX) sites) and expanded with additional sites (e.g., Gavia Pass in the Italian Alps and three sites in Sweden) and years (e.g., 2015 survey data added for Iceland sites, QHI, and Alexandra Fiord; Table S2). We included only sites for which community composition data were roughly equivalent to percent cover (i.e., excluding estimates approximating biomass), for a total of 117 sites (defined as plots in a single contiguous vegetation type) within 38 regions (defined as a CRU[41] grid cell). Plot-level surveys of species composition and cover were conducted at each of these sites between 1989 and 2015 (see[2] for more details of data collection and processing). On average, there were 15.2 plots per site. Repeat surveys were conducted over a minimum duration of 5 and up to 21 years between 1989 and 2015 (mean duration = 13.6 years), for a total of 1,781 unique plots and 5,507 plot-year combinations. Plots were either permanent (i.e., staked; 62% of sites) or semi-permanent (38%), such that the approximate but not exact location was resurveyed. The vegetation monitoring sites were located in tree-less Arctic or alpine tundra and ranged in latitude from 40° (Colorado Rockies) to 80° (Ellesmere Island, Canada) and were circumpolar in distribution (Fig. 1a, Table S2). Our analyses only include vascular plants because there was insufficient trait data for non-vascular species. Changes in bryophytes and other cryptogams are an important part of the trait and function change in tundra ecosystems[42,43], thus the incorporation of non-vascular plants and their traits is a future research priority.

Temperature extraction for community composition observations

We extracted summer (warmest quarter) and winter (coldest quarter) temperature estimates for each of the vegetation survey sites from both the WorldClim[44] (for long-term averages; http://www.worldclim.org/) and CRU[41] (for temporal trends; http://www.cru.uea.ac.uk/) gridded climate datasets. WorldClim temperatures were further corrected for elevation (based on the difference between the recorded elevation of a site and the mean elevation of the WorldClim grid cell) according to a correction factor of -0.005 °C per meter increase in elevation. This correction factor was calculated by extracting the mean temperature and elevation (WorldClim 30s resolution maps) of all cells falling in a 2.5 km radius buffer around our sites and fitting a linear mixed model (with site as a random effect) to estimate the rate of temperature change with elevation.

The average long-term (1960-present) temperature trend across all sites was 0.26 (range -0.06 to 0.49) and 0.43 (range -0.15 to 1.32) °C/decade for summer and winter temperature, respectively.

Soil moisture for community composition observations

A categorical measure of soil moisture at each site was provided by every site PI according to the methods described in Elmendorf et al. 2012 and Myers-Smith et al. 2015 ([2,45]). Soil moisture was considered to be 1) dry when during the warmest month of the year the top 2 cm of the soil was dry to the touch, 2) moist when soils were moist year round, but standing water was not present, and 3) wet when standing water was present during the warmest month of the year.

Soil moisture change for maps of environmental and trait change (Fig. 4b-e)

We used high-resolution soil moisture observations from ESA CCI SM v04.2. To calculate the mean distribution of soil moisture, we averaged the observations from 1979-2016. Because the ESA CCI SM temporal coverage is poor for our sites, temporal data were instead taken from ERA-Interim (Volumetric soil water layer 1) for the same time period. We downscaled the ERA-Interim data to the 0.05° resolution of ESA CCI SM v04.2 using climatologically aided interpolation (delta change method)[46]. The change in soil water content was then calculated separately for each grid cell using linear regression with month as a predictor variable. To classify the soil moisture data into three categories (wet, mesic, dry) to match the community composition dataset, we used a quantile approach on the mean soil moisture within the extent of the Arctic. We assigned the lowest quantile to dry and the highest to wet conditions. For the trends in soil moisture between 1979-2016 we calculated the percentage in change in relation to the mean first, and then calculated the change based on the categorical data (e.g. 5% change from category 1 (dry) to category 2 (mesic)).

Changes in water availability for analysis

Although the strong effect of soil moisture on spatial temperature-trait relationships suggests that change in water availability over time will play an important role in mediating trait change, we did not use the CRU estimates of precipitation change over time because of issues with precipitation records at high latitudes and the inability of gridded datasets to capture localized precipitation patterns (e.g., [47,48]). The CRU precipitation trends at our sites included many data gaps filled by long-term mean values, especially at the high-latitude sites[45]. As a purely exploratory analysis, we used the downscaled ERA-Interim data described above to investigate whether trait change is related to summer soil moisture change (June, July, and August; Extended Data Fig. 5b). However, we caution that soil moisture change in our tundra sites is primarily controlled by snow melt timing, soil drainage, the permafrost table and local hydrology[25], and as such precipitation records and coarse-grain remotely sensed soil moisture change data are unlikely to accurately represent local changes in soil water availability. For this same reason we did not use the ERA-Interim data to explore spatial relationships between temperature, moisture and community traits, as the categorical soil moisture data (described above) were collected specifically within each community composition site and are therefore a more accurate representation of long-term mean soil moisture conditions in that specific location.

TRAIT DATA

Continuous trait data (adult plant height, leaf area (average one-sided area of a single leaf), specific leaf area (leaf area per unit of leaf dry mass; SLA), leaf nitrogen content (per unit of leaf dry mass; leaf N), and leaf dry matter content (leaf dry mass per unit of leaf fresh mass; LDMC); Fig. 1a & Extended Data Fig. 1a, Table S1) were extracted from the TRY[49] 3.0 database (available at www.try-db.org). We also ran a field & data campaign in 2014-15 to collect additional in-situ tundra trait data (the “Tundra Trait Team” (TTT) dataset[50]) to supplement existing TRY records. All species names from the vegetation monitoring sites, TRY and TTT were matched to accepted names in The Plant List using the R package Taxonstand[51] (v. 1.8) before merging the datasets. Community-level traits (woodiness and evergreenness) were derived from functional group classifications for each species[2]. Woodiness is estimated as the proportion (abundance) of woody species in the plot, while evergreenness is the proportion of evergreen woody species abundance out of all woody species (evergreen plus deciduous) in a plot. Because some sites did not contain any woody species (and thus the proportion of evergreen woody species could not be calculated), this trait is estimated only for 98 of the 117 total sites.

Data cleaning - TRY

TRY trait data were subjected to a multi-step cleaning process. First, all values that did not represent individual measurements or approximate species means were excluded. When a dataset within TRY contained only coarse plant height estimates (e.g., estimated to the nearest foot), we removed these values unless no other estimate of height for that species was available. We then identified overlapping datasets within TRY and removed duplicate observations whenever possible. The following datasets were identified as having partially overlapping observations: GLOPNET – Global Plant Trait Network Database, The LEDA Traitbase, Abisko & Sheffield Database, Tundra Plant Traits Database, and KEW Seed Information Database (SID).

We then removed duplicates within each TRY dataset (e.g., if a value is listed once as "mean" and again as "best estimate") by first calculating the ratio of duplicated values within each dataset, and then removing duplicates from datasets with more than 30% duplicated values. This cutoff was determined by manual evaluation of datasets at a range of thresholds. Datasets with fewer than 30% duplicated values were not cleaned in this way as any internally duplicate values were assumed to be true duplicates (i.e., two different individuals were measured and happened to have the same measurement value).

We also removed all species mean observations from the "Niwot Alpine Plant Traits" database and replaced it with the original individual observations as provided by M.J. Spasojevic.

Data cleaning – TRY & TTT combined

Both datasets were checked for improbable values, with the goal of excluding likely errors or measurements with incorrect units but without excluding true extreme values. We followed a series of data-cleaning steps, in each case identifying whether a given observation (x) was likely to be erroneous (i.e. "error risk") by calculating the difference between x and the mean (excluding x) of the taxon and then dividing by the standard deviation of the taxon.

We employed a hierarchical data cleaning method, because the standard deviation of a trait value is related to the mean and sample size. First, we checked individual records against the entire distribution of observations of that trait and removed any records with an error risk greater than 8 (i.e., a value more than 8 standard deviations away from the trait mean). For species that occurred in four or more unique datasets with TRY or TTT (i.e., different data contributors), we estimated a species mean per dataset and removed observations for which the species mean error risk was greater than 3 (i.e., the species mean of that dataset was more than 3 SD's away from the species mean across all datasets). For species that occurred in fewer than 4 unique datasets, we estimated a genus mean per dataset and removed observations in datasets for which the error risk based on the genus mean was greater than 3.5. Finally, we compared individual records directly to the distribution of values for that species. For species with more than 4 records, we excluded values above an error risk Y, where Y was dependent on the number of records of that species and ranged from an error risk of 2.25 for species with fewer than 10 records to an error risk of 4 for species with more than 30 records. For species with four or fewer records, we manually checked trait values and excluded only those that were obviously erroneous, based on our expert knowledge of these species.

This procedure was performed on the complete tundra trait database – including species and traits not presented here. In total 2,056 observations (1.6%) were removed. In all cases, we visually checked the excluded values against the distribution of all observations for each species to ensure that our trait cleaning protocol was reasonable.

Trait data were distributed across latitudes within the tundra biome (Extended Data Fig. 1a). All trait observations with latitude/longitude information were mapped and checked for implausible values (e.g., falling in the ocean). These values were corrected from the original publications or by contacting the data contributor whenever possible.

Final trait database

After cleaning out duplicates and outliers as described above, we retained 56,048 unique trait observations (of which 18,613 are contained in TRY and 37,435 were newly contributed by the Tundra Trait Team[50] field campaign) across the five traits of interest. Of the 447 identified species in the ITEX dataset, 386 (86%) had trait data available from TRY or TTT for at least one trait (range 52-100% per site). Those species without trait data generally represent rare or uncommon species unique to each site; on average, trait data were available for 97% of total plant cover across all sites (range 39-100% per site; Table S1).

Temperature extraction for trait observations

WorldClim climate variables were extracted for all trait observations with latitude/longitude values recorded (53,123 records in total, of which 12,380 were from TRY and 33,621 from TTT). Because most observations did not include information about elevation, temperature estimates for individual trait observations were not corrected for elevation and thus represent the temperature at the mean elevation of the WorldClim grid cell.

ANALYSES

Terminology

Here we provide a brief description of acronyms and symbols used in the methods and model equations.

ITV – intraspecific trait variation: variation in trait values within the same species
CWM – community weighted trait mean: the mean trait value of all species in a plot, weighted by their abundance in the plot
CWM + ITV – community weighted trait mean, adjusted with the estimated contribution of intraspecific trait variation based on the intraspecific temperature-trait relationship of each species
α – alpha, used to designate lower-level model intercepts
β – beta, used to designate lower-level model slopes
γ – gamma, used to designate the model parameters of interest (e.g. the temperature-trait relationship)

Models

All analyses were conducted in JAGS and/or Stan through R (v. 3.3.3) using packages *rjags*[52] (v. 4.6) and *rstan*[53] (v. 2.14.1). In all cases, models were run until convergence was reached, as assessed both visually in traceplots and by ensuring that all Gelman-Rubin convergence diagnostic (Rhat[54]) values were less than 1.1.

A major limitation of the species mean trait approach often employed in analyses of environment-trait relationships has been the failure to account for intraspecific trait variation (ITV) that could be as or more important than interspecific variation[55,56]. We addressed this issue by employing a hierarchical analysis that incorporates both within-species and community-level trait variation across climate gradients to estimate trait change over space and time at the biome scale. We used a Bayesian approach that accounts for the hierarchical spatial (plots within sites within regions) and taxonomic (intra- and inter-specific variation) structure of the data as well as uncertainty in estimated parameters introduced through absences in trait records for some species, and taxa that were identified to genus or functional group (rather than species) in vegetation surveys.

Intraspecific trait variation

We subsetted the trait dataset to just those species for which traits had been measured in at least four unique locations spanning a temperature range of at least 10% of the entire temperature range (2.6°C and 5.0 °C for summer and winter temperature, respectively), and for which the latitude and longitude of the measured individual or group of individuals was recorded. The number of species meeting these criteria varied by trait and temperature variable: 108-109 for SLA, 80-86 for plant height, 74-72 for leaf nitrogen, 85-76 for leaf area, and 43-52 for LDMC, for summer and winter temperature, respectively. These species counts correspond to 53-73% of community abundance. The relationship between each trait and temperature (Fig. 2b) was estimated from a Bayesian hierarchical model, with temperature as the predictor variable and species (*s*) and dataset-by-location (*d*) modeled as random effects:

$$traitobs_i \sim logNormal(\alpha_{s,d}, \sigma_s)$$
$$\alpha_{s,d} \sim Normal(\alpha_s + \beta_s \cdot temperature_d, \sigma_1)$$
$$\beta_s \sim Normal(\mathrm{B}, \sigma_2)$$
$$\alpha_s \sim Normal(\mathrm{A}, \sigma_3)$$

where i represents each trait observation and A and B are the intercept and slope hyperparameters, respectively. Because LDMC represents a ratio and is thus bound between 0 and 1, we used a beta error distribution for this trait. Temperature values were mean-centered within each species. We used non-informative priors for all coefficients.

We further explored whether the strength of intraspecific temperature-height relationships varied by functional group. We find that all functional groups (including dwarf shrubs, which are genetically limited in their ability to grow upright) show similar temperature-trait relationships (Extended Data Fig. 9a). These results suggest that the intraspecific temperature-trait relationships may not only be a response of individual growth changes, and are not restricted to particular functional groups with greater capacity for vertical growth (e.g., tall shrubs and graminoids versus dwarf shrubs and certain forb species).

Calculation of community weighted mean (CWM) values

We calculated the community-weighted trait mean (i.e., the mean trait value of all species in a plot, weighted by the abundance of each species), for all plots within a site. We employed a Bayesian approach to calculate trait means for every species (*s*) using an intercept-only model (such that the intercept per species (α_s) is equivalent to the mean trait value of the species) and variation per species (σ_s) with a lognormal error distribution.

$$traitobs_i \sim logNormal(\alpha_s, \sigma_s)$$

Because LDMC represents a ratio and is thus bound between 0 and 1, we used a beta error distribution instead of lognormal for this trait. When a species was measured multiple times in several different locations, we additionally included a random effect of dataset-by-location (*d*) to reduce the influence of a single dataset with many observations at one site when calculating the mean per species:

$$traitobs_i \sim logNormal\left(\alpha_{s,d}, \sigma_d\right)$$
$$\alpha_{s,d} \sim Normal(\alpha_s, \sigma_s)$$

We used non-informative priors for all species intercept parameters for which there were four or more unique trait observations, so that the species-level intercept and variance around the intercept per species were estimated from the data. In order to avoid removing species with little or no trait data from the analyses, we additionally employed a "gap-filling" approach that allowed us to estimate a species' trait mean while accounting for uncertainty in the estimation of this mean. For species with fewer than four but more than one trait observation, we used a normal prior with the mean equal to the mean of the observation(s) and variance estimated based on the mean mean-variance ratio across all species. In other words, we calculated the ratio of mean trait values to the standard deviation of those trait values per species for all species with greater than four observations, then took the mean of these ratios across all species and multiplied this number by the mean of species X (where X is a species with 1-4 observations) to get the prior for σ. For species with no observations (see Table S1), we used a prior mean equal to the mean of all species in the same genus and a prior variance estimated based on the mean mean-variance ratio of all species in that genus or 1.5 times the mean, whichever was lower. If there were no other species in the same genus, then we used a prior mean equal to the mean of all other species in the family and a prior variance estimated based on the mean mean-variance ratio of all species in the family or 1.5 times the mean, whichever was lower.

Calculation of CWM values: incorporating uncertainty in species traits

In order to include uncertainty about species trait means (due to intraspecific trait variation, missing trait information for some species, or when taxa were identified to genus or functional group rather than species) in subsequent analyses, we estimated community-level trait values per plot by sampling from the posterior distribution (mean +/- SD) of each species intercept estimate and multiplying this distribution by the relative abundance of each species in the plot to get a community-weighted mean (CWM) distribution per plot (p):

$$Normal(CWMmean_p, CWMsd_p)$$

This approach generates a distribution of CWM values per plot that propagates the uncertainty in each species' trait mean estimate into the plot-level (CWM) estimate. By using a Bayesian approach, we are able to carry through uncertainty in trait mean estimates to all subsequent analyses and reduce the potential for biased or deceptively precise estimates due to missing trait observations.

Calculation of CWM values: partitioning turnover and estimating contribution of ITV

To assess the degree to which the spatial temperature-trait relationships are caused by species turnover versus shifts in abundance among sites, we repeated each analysis using the non-weighted community mean (all species weighted equally) of each plot. Temperature-trait relationships estimated with non-weighted community means are due solely to species turnover across sites. Finally, we assessed the potential contribution of intraspecific trait variation (ITV) to the community-level temperature-trait relationship by using the modeled intraspecific temperature-trait relationship (described above) to predict trait "anomaly" values for each species at each site based on the temperature of that site in a given year relative to its long-term average.

An intraspecific temperature-trait relationship could not be estimated for every species due to an insufficient number of observations for some species. Therefore, we used the mean intraspecific temperature-trait slope across all species to predict trait anomalies for species without intraspecific temperature-trait relationships. These site- and year-specific species trait estimates were then used to calculate "ITV-adjusted" community-weighted means (CWM+ITV) for each plot in each year measured, and modeled as for CWM alone. As these "adjusted" values are estimated *relative to each species' mean value*, the spatial temperature-trait relationship that includes this adjustment does not remove any bias in the underlying species mean data. For example, if southern tundra species tend to be measured at the southern edge of their range while northern tundra species tend to be measured at the northern edge of their range, the overall spatial temperature-trait relationship could appear stronger than it really is for species with temperature-related intraspecific variation. This is a limitation of any species-mean approach.

Estimates of temporal CWM+ITV temperature-trait relationships are not prone to this same limitation as they represent relative change, but should also be interpreted with caution as intraspecific temperature-trait relationships may be due to genetic differences among populations rather than plasticity, thus suggesting that trait change would not occur immediately with warming. We therefore caution that the CWM+ITV analyses presented here represent estimates of the potential contribution of ITV to overall CWM temperature-trait relationships over space and time, but should not be interpreted as measured responses.

In sum, we incorporate intraspecific variation into our analyses in three ways. First, by using the posterior distribution (rather than a single mean value) of species trait mean estimates in our calculations of CWM values per plot, so that information about the amount of variation within species is incorporated into all the analyses in our study. Second, by explicitly estimating intraspecific temperature-trait relationships based on the spatial variation in individual trait observations. And finally, by using these modeled temperature-trait relationships to inform estimates of the potential contribution of ITV to overall (CWM+ITV) temperature-trait relationships over space and time.

Spatial community trait models (Fig. 2 a&c)

To investigate spatial relationships in plant traits with summer and winter temperature and soil moisture we used a Bayesian hierarchical modeling approach in which soil moisture and soil moisture x temperature vary at the site level while temperature varies by WorldClim region (unique WorldClim grid x elevation groups). In total, there were 117 sites (*s*) nested within 73 WorldClim regions (*r*). We used only the first year of survey data at each site to estimate spatial relationships in community traits.

$$CWMmean_p \sim Normal(\alpha_s + \alpha_r, CWMsd_p)$$

$$\alpha_s \sim Normal(\gamma_1 \cdot moisture_s + \gamma_2 \cdot moisture_s \cdot temperature_s, \sigma_1)$$

$$\alpha_r \sim Normal(\gamma_0 + \gamma_3 \cdot temperature_r, \sigma_2)$$

Where $CWMmean_p$ is the mean of the posterior distribution of the community-weighted mean (CWM) estimate per plot (*p*) and $CWMsd_p$ is the standard deviation of the posterior distribution of the CWM estimate per plot, as described in the "*Calculation of CWM values: incorporating uncertainty in species traits*" section. See supplementary information for complete STAN code.

As woodiness and evergreenness represent proportional data (bounded between 0 and 1, inclusive), we used a beta-Bernoulli mixture model of the same structure as above to estimate trait-temperature-moisture relationships for these traits (Extended Data Fig. 3 a&b). The discrete and continuous components of the data were modeled separately, with mixing occurring at the site- and region-level estimates (α_s and α_r).

Because Arctic and alpine tundra sites might differ in their trait-environment relationships due to environmental differences in e.g. soil drainage, we also performed a version of the spatial community trait analyses in which the elevation of each site is visually indicated (not modeled; Extended Data Fig. 9b). We did not attempt to separately analyze trait-environment relationships for Arctic and alpine sites due to the ambiguity in defining this cut-off (i.e., many sites can be categorized as both Arctic and alpine, particularly in Scandinavia and Iceland) and because of the small number of southern, high-alpine sites (European Alps and Colorado Rockies).

For estimation of the overall temperature-trait relationship, we used a model structure similar to that above but with only temperature as a predictor (i.e., without soil moisture). This model was used for both community-weighted mean (CWM) and non-weighted mean estimates in order to determine the degree to which temperature-trait relationships over space are due to species turnover alone (non-weighted mean) and for CWM+ITV plot-level estimates to determine the likely additional contribution of intraspecific trait variation to the overall temperature-trait relationship, as described above.

Standardized effect sizes for CWM temperature-trait relationships (Fig. 2c) were obtained by dividing the slope of the temperature-trait relationship by the standard deviation of the CWM model residuals. Effect sizes for ITV, turnover only, and CWM: ITV were estimated relative to the CWM value for that same trait based on the slope values of each temperature-trait relationship.

Trait change over time (Fig. 3 a&b)

Change over time was modeled at the CRU grid cell (region) level (*r*), with site (*s*) as a random effect when there was more than one site per region (to account for non-independence of sites within a region) and plot (*p*) as a random effect for those sites with permanent (repeating) plots (to account for repeated measures on the same plot over time). We did not account for temporal autocorrelation as most plots were not measured annually (average survey interval = 7.2 years) and did not have more than 3 observations over the study period (average number of survey years per plot = 3.1). Year (y) was centered within each region.

$$CWMmean_{p,y} \sim Normal(\alpha_p + \alpha_s + \alpha_{r,y}\,, CWMsd_{p,y})$$

Where $CWMmean_p$ is the mean of the posterior distribution of the community-weighted mean (CWM) estimate per plot (*p*) and $CWMsd_p$ is the standard deviation of the posterior distribution of the CWM estimate per plot, as described in the "*Calculation of CWM values: incorporating uncertainty in species traits*" section. For non-permanent plots and for sites that were the only site within a region, α_p or α_s, respectively, were set to 0. Region-level slopes were then used to fit an average trend of community trait values over time:

$$\alpha_{r,y} \sim Normal(\alpha_r + \beta_r \cdot year_{y,r}, \sigma_0)$$
$$\beta_r \sim Normal(\mathrm{B}, \sigma_1)$$
$$\alpha_r \sim Normal(\mathrm{A}, \sigma_2)$$

where A and B are the intercept and slope hyperparameters, respectively. See supplementary information for complete STAN code. This model was used for both community-weighted mean (CWM) and non-weighted mean plot-level estimates in order to determine the degree to which temporal trait change is due to species turnover alone (non-weighted mean) and for CWM+ITV plot-level estimates to determine the potential additional contribution of intraspecific trait variation to overall trait change.

Standardized effect sizes for CWM change over time (Fig. 3b) were obtained by dividing the slope of overall trait change over time (mean hyperparameter across 117 sites) by the standard deviation of the slope estimates per site. Effect sizes for turnover-only and CWM+ITV change are estimated relative to the CWM change value for that trait based on the slope values of each.

To estimate change in the proportion of woody and evergreen species over time (CWM change only; Extended Data Fig. 3 c&d) we used a beta-Bernoulli mixture model of the same form described above. The discrete and continuous components of the data were modeled separately, with mixing occurring at the region x year effect ($\alpha_{r,y}$). We additionally assessed whether the rate of observed trait change over time was related to the duration of vegetation monitoring at each site. There was no influence of monitoring duration for any trait (not shown).

Temperature sensitivity (Fig. 3c)

Temperature sensitivity was modeled as the variation in CWM trait values with variation in the five-year mean temperature (i.e., the mean temperature of the survey year and the four preceding years). A four-year lag was chosen because this interval has been shown to best explain vegetation change in tundra[20] and alpine[29] plant communities. The model specifics are exactly as shown above for "Trait change over time", but with temperature in the place of year. Temperatures were centered within each region.

Observed vs. expected trait change (Fig. 4a)

We first calculated the mean rate of temperature change across the 38 regions in our study, and then estimated the *expected* degree of change in each trait over the same period based on this temperature change and the spatial relationship between temperature and CWM trait values (described in the "*Spatial community trait models*" section). We then compared this *expected* trait change to actual trait change over time (described in the "*Trait change over time*" section). To create Fig. 4a we used the overall predicted mean value of each trait in the first year of survey (1989) as an intercept, and then used the expected and observed rates of trait change (+/- uncertainty) to predict community trait values in each year thereafter. We subtracted the intercept from all predicted values in order to show trait change as an anomaly (difference from 0). The difference between the expected (black) and observed (colored) lines in Fig. 4a represents a deviation from expected. To calculate total trait change including the estimated contribution of intraspecific change (colored dashed lines), we followed the same procedure as described for "observed" trait change but where this observed change was based on plot-level CWM+ITV estimates that varied by year based on the temperature in that year and the temperature-trait relationship per species (described in the "*Calculation of CWM values: partitioning turnover and estimating contribution of ITV*" section).

Trait change vs. temperature change and soil moisture (Extended Data Fig. 5)
To determine whether the rate of trait change can be explained by the rate of temperature change at a site, the (static) level of soil moisture of a site, or their interaction, we modeled the rate of trait change as described above ("Trait change over time") and compared it to the rate of temperature change over the same time interval (with a lag of four years) and soil moisture:

$$\beta_r \sim Normal(\gamma_0 + \gamma_1 \cdot temp_r + \gamma_2 \cdot moisture_r + \gamma_3 \cdot temp_r \cdot moisture_r, \sigma)$$

where β_r is the rate of trait change per region (Extended Data Fig. 5a). When sites within a region were measured over different intervals or contained different soil moisture estimates they were modeled separately in order to match with temperature change estimates over the same interval and soil moisture estimates, which vary at the site level.

We also conducted this analysis using estimates of soil moisture change (with a lag of four years) from downscaled ERA-Interim (volumetric soil water layer 1). This model took the same form as above, but with moisture change in place of static soil moisture estimates (Extended Data Fig. 5b). Trait change was modeled at the site (rather than region) level because estimates of soil moisture change vary at the site level. Because ERA-Interim data were not available for every site, this analysis was conducted with a total of 101 rather than 117 sites. We note that the results of this analysis should be interpreted cautiously, as local changes in soil moisture may not be well represented by coarse-scale remotely sensed data, as described previously.

Species gains and losses as a function of traits (Extended Data Fig. 6)
We estimated species gains and losses at the site (rather than plot) level to reduce the effect of random fluctuations in species presences/absences due to observer error. Thus, sites with repeating and non-repeating plots were treated the same. A "gain" was defined as a species that did not occur in a site in the first survey year but did in the last survey year, while a "loss" was the reverse. We then modeled the probability of gain or loss separately as a function of the mean trait value of each species. For example, for "gains," all newly

observed species received a response type of 1 while all other species in the site received a response type of 0:

$$response_i \sim Bernoulli(\alpha_s + \alpha_r + \beta_r \cdot trait_i)$$
$$\alpha_r \sim Normal(A, \sigma_1)$$
$$\beta_r \sim Normal(B, \sigma_2)$$
$$\alpha_s \sim Normal(0, \sigma_r)$$

We included a random effect for site (s) only when there were multiple sites within the same region (r), otherwise α_s was set to 0. We considered species' responses to be related to a given trait when the 95% credible interval on the slope hyperparameter (B) did not overlap zero.

Trait projections with warming (Extended Data Fig. 7)

We projected trait change for the minimum (RCP2.6) and maximum (RCP8.5) IPCC carbon emission scenarios from the NIMR HadGEM2-AO Global Circulation Model. We used the midpoint years of the WorldClim (1975) and HadGem2 (2090) estimates to calculate the expected rate of temperature change over this time period. We then predicted trait values for each year into the future based on the projected rate of temperature change and the spatial relationship between temperature and community trait values (described in the "*Spatial community trait models*" section).

These projections are not intended to predict actual expected trait change over the next century, as many other factors not accounted for here will also influence this change. In particular, future changes in functional traits will likely depend on concurrent changes in moisture availability, which are less well understood than temperature change. Recent modeling efforts predict increases in precipitation across much of the Arctic[57], but it is unknown whether increasing precipitation will also lead to an increase in soil moisture/water availability for plants, as the drying effect of warmer temperatures (e.g. due to increased evaporation and/or decreased duration of snow cover[58]) may outweigh the impact of increased precipitation. Instead, these projections are an attempt to explore theoretical trait change over the long-term when using a space-for-time substitution approach.

Principal component analysis (PCA; Extended Data Fig. 8)

We performed an ordination of community-weighted trait mean values per plot on all seven traits. Because community evergreenness could only be estimated for plots with at least one woody species, the total number of plots included in this analysis is reduced compared to the entire dataset (1098 plots out of 1520 in total). We used the R package *vegan*[59] (v. 2.4.6) to conduct a principal component analysis of these data. This analysis uses only trait means per plot, and therefore information about CWM uncertainty due to intraspecific trait variation and/or missing species is lost. The analysis was performed on log-transformed trait values[49]. We extracted the axis coordinates of each plot from the PCA and used the spatial trait-temperature-moisture model described above (section "*Spatial community trait models*") to determine whether plot positions along both PCA axes varied with temperature, moisture, and their interaction.

Trends in species abundance (Supplementary Information, Table S10)

In order to provide more insight into the species-specific changes occurring over time in tundra ecosystems, we calculated trends in abundance for the most common (widespread and abundant) species in the community composition dataset. We estimated trends for all species that occurred in at least 5 sites at a minimum abundance of 5% cover (mean of all plots within a site) across all years. We additionally included species that occurred at low abundance (1% or more) but were widespread (at least 10 sites). This technique yielded a total of 79 species. Abundance changes were modeled as described for trait change over time, but because abundance (proportion of plot cover) is bounded between 0 and 1, inclusive, we used a beta-Bernoulli mixture model. Abundance change was then estimated per species (sp) across all regions (r):

$$\alpha_{sp,r,y} \sim Normal(\alpha_{sp,r} + \beta_{sp,r} \cdot year_{sp,r,y}, \sigma_{sp})$$
$$\beta_{sp,r} \sim Normal(\mathrm{B}_{sp}, \sigma_1)$$
$$\alpha_{sp,r} \sim Normal(\mathrm{A}_{sp}, \sigma_2)$$

We additionally extracted region-specific slopes per species ($\beta_{sp,r}$) in order to calculate a proportion of regions in which a given species was increasing or decreasing ("Prop. Increase" and "Prop. Decrease" in Table S10). Because regional slopes are modeled as random effects, these estimates are not entirely independent (i.e., they will be pulled toward the overall species mean slope), but provide an approximate estimate of whether directional trends in abundance are consistent across a species' range.

Methods References

41. Harris, I., Jones, P. D., Osborn, T. J. & Lister, D. H. Updated high-resolution grids of monthly climatic observations – the CRU TS3.10 Dataset. *International Journal of Climatology* **34,** 623–642 (2014).
42. Blok, D. *et al.* The Cooling Capacity of Mosses: Controls on Water and Energy Fluxes in a Siberian Tundra Site. *Ecosystems* **14,** 1055–1065 (2011).
43. Soudzilovskaia, N. A., van Bodegom, P. M. & Cornelissen, J. H. C. Dominant bryophyte control over high-latitude soil temperature fluctuations predicted by heat transfer traits, field moisture regime and laws of thermal insulation. *Functional Ecology* **27,** 1442–1454 (2013).
44. Hijmans, R. J., Cameron, S. E., Parra, J. L., Jones, J. L. & Jarvis, A. Very high resolution interpolated climate surfaces for global land areas. *International Journal of Climatology* **25,** 1965–1978 (2005).
45. Myers-Smith, I. H. *et al.* Climate sensitivity of shrub growth across the tundra biome. *Nature Climate Change* **5,** 887–891 (2015).
46. Willmott, C. J. & Robeson, S. M. Climatologically aided interpolation (CAI) of terrestrial air temperature. *International Journal of Climatology* **15,** 221–229 (1995).
47. Sperna Weiland, F. C., Vrugt, J. A., van Beek, R. L.). P. H., Weerts, A. H. & Bierkens, M. F. P. Significant uncertainty in global scale hydrological modeling from precipitation data errors. *Journal of Hydrology* **529,** 1095–1115 (2015).
48. Beguería, S., Vicente Serrano, S. M., Tomás Burguera, M. & Maneta, M. Bias in the variance of gridded data sets leads to misleading conclusions about changes in climate variability. *International Journal of Climatology* **36,** 3413–3422 (2016).
49. Kattge, J. *et al.* TRY–a global database of plant traits. *Global Change Biology* **17,** 2905–2935 (2011).
50. Bjorkman, A. D. *et al.* Tundra Trait Team: A database of plant traits spanning the tundra biome. *Global Ecology and Biogeography*
51. Cayuela, L., Granzow-de la Cerda, Í., Albuquerque, F. S. & Golicher, D. J. TAXONSTAND: An R package for species names standardisation in vegetation databases. *Methods in Ecology and Evolution* **3,** 1078–1083 (2012).
52. Plummer, M. rjags: Bayesian graphical models using MCMC. (2016).
53. Stan Development Team. RStan: the R interface to Stan. (2016).
54. Gelman, A. & Rubin, D. B. Inference from iterative simulation using multiple sequences. *Statistical Science* **7,** 457–472 (1992).

55. Messier, J., McGill, B. J. & Lechowicz, M. J. How do traits vary across ecological scales? A case for trait-based ecology. *Ecology Letters* **13,** 838–848 (2010).
56. Violle, C. *et al.* The return of the variance: intraspecific variability in community ecology. *Trends Ecol. Evol.* **27,** 245–253 (2012).
57. Bintanja, R. & Selten, F. M. Future increases in Arctic precipitation linked to local evaporation and sea-ice retreat. *Nature* **509,** 479–482 (2014).
58. AMAP. *Snow, Water, Ice and Permafrost in the Arctic (SWIPA) 2017*. (Arctic Monitoring and Assessment Programme (AMAP), 2017).
59. Oksanen, J., Blanchet, F., Kindt, R. & Legendre, P. Package 'vegan'. (2011).
60. Chapin, F. S., III, BretHarte, M. S., Hobbie, S. E. & Zhong, H. L. Plant functional types as predictors of transient responses of arctic vegetation to global change. *Journal of Vegetation Science* **7,** 347–358 (1996).
61. Weiher, E. *et al.* Challenging Theophrastus: A Common Core List of Plant Traits for Functional Ecology. *Journal of Vegetation Science* **10,** 609–620 (1999).
62. Violle, C. *et al.* Let the concept of trait be functional! *Oikos* **116,** 882–892 (2007).
63. Hudson, J. M. G. & Henry, G. H. R. Increased plant biomass in a High Arctic heath community from 1981 to 2008. *Ecology* **90,** 2657–2663 (2009).
64. De Deyn, G. B., Cornelissen, J. H. C. & Bardgett, R. D. Plant functional traits and soil carbon sequestration in contrasting biomes. *Ecology Letters* **11,** 516–531 (2008).
65. Kunstler, G. *et al.* Plant functional traits have globally consistent effects on competition. *Nature* **529,** 204–207 (2016).
66. Gaudet, C. L. & Keddy, P. A. A Comparative Approach to Predicting Competitive Ability From Plant Traits. *Nature* **334,** 242–243 (1988).
67. Westoby, M., Falster, D. S., Moldes, A. T., Vesk, P. A. & WRIGHT, I. J. Plant ecological strategies: Some leading dimensions of variation between species. *Annual Review of Ecology and Systematics* **33,** 125–159 (2002).
68. Moles, A. T. & Leishman, M. R. *Seedling Ecology and Evolution*. (Cambridge University Press, 2008).
69. Sturm, M. *et al.* Snow-shrub interactions in Arctic tundra: a hypothesis with climatic implications. *Journal of Climate* **14,** 336–344 (2001).
70. Loranty, M. M., Berner, L. T., Goetz, S. J., Jin, Y. & Randerson, J. T. Vegetation controls on northern high latitude snow-albedo feedback: observations and CMIP5 model simulations. *Global Change Biology* **20,** 594–606 (2014).

71. Myers-Smith, I. H. & Hik, D. S. Shrub canopies influence soil temperatures but not nutrient dynamics: An experimental test of tundra snow-shrub interactions. *Ecol Evol* **3,** 3683–3700 (2013).

72. DeMarco, J., Mack, M. C. & Bret-Harte, M. S. Effects of arctic shrub expansion on biophysical vs. biogeochemical drivers of litter decomposition. *Ecology* **95,** 1861–1875 (2014).

73. Enquist, B. J., Brown, J. H. & West, G. B. Allometric scaling of plant energetics and population density. *Nature* **395,** 163–165 (1998).

74. Street, L. E., Shaver, G. R., Williams, M. & van Wijk, M. T. What is the relationship between changes in canopy leaf area and changes in photosynthetic CO2 flux in arctic ecosystems? *Journal of Ecology* **95,** 139–150 (2007).

75. Poorter, H. *et al.* Biomass allocation to leaves, stems and roots: meta-analyses of interspecific variation and environmental control. *New Phytol.* **193,** 30–50 (2012).

76. Greaves, H. E. *et al.* Estimating aboveground biomass and leaf area of low-stature Arctic shrubs with terrestrial LiDAR. *Remote Sensing of Environment* **164,** 26–35 (2015).

77. Westoby, M. & Wright, I. J. Land-plant ecology on the basis of functional traits. *Trends Ecol. Evol.* **21,** 261–268 (2006).

78. Niinemets, Ü. A review of light interception in plant stands from leaf to canopy in different plant functional types and in species with varying shade tolerance. *Ecological Research* **25,** 693–714 (2010).

79. Freschet, G. T., Aerts, R. & Cornelissen, J. H. C. A plant economics spectrum of litter decomposability. *Functional Ecology* **26,** 56–65 (2012).

80. Manning, P. *et al.* Simple measures of climate, soil properties and plant traits predict national-scale grassland soil carbon stocks. *Journal of Applied Ecology* **52,** 1188–1196 (2015).

81. Lida, Y. *et al.* Wood density explains architectural differentiation across 145 co-occurring tropical tree species. *Functional Ecology* **26,** 274–282 (2012).

82. Ménard, C. B., Essery, R., Pomeroy, J., Marsh, P. & Clark, D. B. A shrub bending model to calculate the albedo of shrub-tundra. *Hydrological Processes* **28,** 341–351 (2014).

83. Nauta, A. L. *et al.* Permafrost collapse after shrub removal shifts tundra ecosystem to a methane source. *Nature Climate Change* **5,** 67–70 (2015).

84. Hobbie, S. E. Temperature and Plant Species Control Over Litter Decomposition in Alaskan Tundra. *Ecological Monographs* **66,** 503–522 (1996).

85. Weedon, J. T. *et al.* Global meta-analysis of wood decomposition rates: a role for trait variation among tree species? *Ecology Letters* **12,** 45–56 (2009).
86. Dorrepaal, E., Cornelissen, J., Aerts, R., Wallen, B. & Van Logtestijn, R. Are growth forms consistent predictors of leaf litter quality and decomposability across peatlands along a latitudinal gradient? *Journal of Ecology* **93,** 817–828 (2005).
87. Larsen, K. S., Michelsen, A., Jonasson, S., Beier, C. & Grogan, P. Nitrogen Uptake During Fall, Winter and Spring Differs Among Plant Functional Groups in a Subarctic Heath Ecosystem. *Ecosystems* **15,** 927–939 (2012).
88. Chapin, F. S., III, Shaver, G. R., Giblin, A. E., Nadelhoffer, K. J. & Laundre, J. A. Responses of arctic tundra to experimental and observed changes in climate. *Ecology* **76,** 694–711 (1995).
89. Reich, P. B., Walters, M. B. & Ellsworth, D. S. From tropics to tundra: Global convergence in plant functioning. *Proceedings of the National Academy of Sciences* **94,** 13730–13734 (1997).
90. Dornelas, M. *et al.* BioTIME: A database of biodiversity time series for the Anthropocene. *Global Ecology and Biogeography* **27,** 760–786 (2018).

DATA AVAILABILITY

Trait data

Data compiled through the Tundra Trait Team are publicly accessible[50] (data paper published in Global Ecology & Biogeography). The public TTT database includes traits not considered in this study as well as tundra species that do not occur in our vegetation survey plots, for a total of nearly 92,000 trait observations on 978 species. Additional trait data from the TRY trait database can be requested at try-db.org.

Composition data

Most sites and years of the vegetation survey data included in this study are available in the Polar Data Catalogue (ID # 10786_iso). Much of the individual site-level data has additionally been made available in the BioTIME database[90] (https://synergy.st-andrews.ac.uk/biotime/biotime-database/).

References

50. Bjorkman, AD, IH Myers-Smith, SC Elmendorf, S Normand, HJD Thomas, *et al*. Tundra Trait Team: a database of plant traits spanning the tundra biome. Global Ecology and Biogeography. *In press.*

90. Dornelas, M, LH Antão, F Moyes, AE Bates, AE Magurran, *et al*. 2018. BioTIME: A database of biodiversity time series for the Anthropocene. Global Ecology and Biogeography. 27: 760-786.

CODE AVAILABILITY

STAN code for the two main models (spatial temperature-moisture-trait relationships and community trait change over time) is provided in the Supplementary Information associated with this study (available online).

Extended Data Fig. 1. Overview of trait data and analyses. a, Count of traits per latitude (rounded to the nearest degree) for all georeferenced observations in TRY and TTT that correspond to species in the vegetation survey dataset. **b,** Work flow and analyses of temperature-trait relationships. Intraspecific temperature-trait relationships over space were used to estimate the potential contribution of ITV to overall temperature-trait relationships over space and time (CWM + ITV) as trait measurements on individuals over time are not available.

Extended Data Fig. 2. All temperature-trait relationships. Slope of temperature-trait relationship over space (within-species (ITV) and across communities (CWM)) and with interannual variation in temperature (community temperature sensitivity). Spatial – ITV is the average intraspecific trait variation as related to temperature over space, Spatial – CWM is the relationship between community-weighted trait means and summer temperature, and Temporal sensitivity – CWM is the temperature sensitivity of community-weighted trait means (i.e., correspondence between interannual variation in CWM values with interannual variation in temperature). Error bars represent 95% credible intervals on the slope estimate. We used five-year mean temperatures (temperature of the survey year and four previous years) to estimate temperature sensitivity because this interval has been shown to explain vegetation change in tundra[20] and alpine[29] plant communities. All slope estimates are in transformed units (height = log cm, LDMC = logit g/g, leaf area = log cm^2, leaf nitrogen = log mg/g, SLA = log mm^2/mg). Community (CWM) temperature-trait relationships are estimated across all 117 sites; intraspecific temperature-trait relationships are estimated as the mean of 108-109 species for SLA, 80-86 species for plant height, 74-72 species for leaf nitrogen, 85-76 species for leaf area, and 43-52 species for LDMC, for summer and winter temperature, respectively (see *Methods: Analyses: Intraspecific Trait Variation* for details).

Extended Data Fig. 3. Community woodiness and evergreenness over space and time. a-b, Variation in community woodiness (**a**) and evergreenness (**b**) across space with summer temperature and soil moisture. Community woodiness is the abundance-weighted proportion of woody species versus all other plant species in the community. Community evergreenness is the abundance-weighted proportion of evergreen shrubs versus all shrub species (deciduous and evergreen). The evergreen model was conducted on a reduced number of sites (98 instead of 117) because some sites did not have any woody species (and it was thus not possible to calculate a proportion evergreen). Both temperature and moisture were important predictors of community woodiness and evergreenness. The 95% credible interval for a temperature * moisture interaction term overlapped zero in both models (-0.100 to 0.114 and -0.201 to 0.069 for woodiness and evergreenness, respectively). **c-d,** There was no change over time in woodiness (**c**) or evergreenness (**d**). Thin lines represent slopes per site (woodiness: n = 117 sites, evergreenness, n = 98 sites). In all panels, bold lines indicate overall model predictions and shaded ribbons designate 95% credible intervals on these model predictions.

Extended Data Fig. 4. Range in species mean values of each trait by summer temperature. Black dashed lines represent quantile regression estimates for 1% and 99% quantiles. Species mean values are estimated from intercept-only Bayesian models using the estimation technique described in *Methods: Analyses: Calculation of community weighted mean (CWM) values*. Species locations are based on species in the 117 vegetation survey sites. All values are back-transformed into their original units (height = cm, LDMC = g/g, leaf area = cm^2, leaf nitrogen = mg/g, SLA = mm^2/mg).

Extended Data Fig. 5. The rate of community trait change is not related to the rate of temperature change or soil moisture for any trait. a-b, Rate of community-weighted mean change over time per site (N = 117 sites) as related to temperature change and long-term mean soil moisture (**a**) or soil moisture change (**b**) at a site. Points represent mean trait change values for each site, lines represent the predicted relationship between trait change, temperature change and soil moisture/soil moisture change, and transparent ribbons are the 95% CI's on these predictions. Both mean soil moisture and soil moisture change were modeled as a continuous variables, but are shown as predictions for minimum and maximum values/rates of change. Trait change estimates are in transformed units (log for height, leaf area, leaf nitrogen, and SLA, and logit for LDMC). Soil moisture change was estimated from downscaled ERA Interim data and may not accurately represent local changes in moisture availability at each site.

Extended Data Fig. 6. Increasing community height is driven by the immigration of taller species, not the loss of shorter ones. Probability that a species newly arrived in a site ("gained") or disappeared from a site ("lost") as a function of its traits (N = 117 sites). Lines and ribbons represent overall model predictions and the 95% credible intervals on these predictions, respectively. Dark ribbons and solid lines represent species gains while pale ribbons and dashed lines represent species losses. Only for plant height was the trait-probability relationship different for gains and losses.

Extended Data Fig. 7. Comparison of actual (colored lines), expected (solid black lines), and projected (dotted/dashed black lines) CWM trait change over time. Expected trait change is calculated using the observed spatial temperature-trait relationship and the average rate of recent summer warming across all sites. Note that these projections assume no change in soil moisture conditions. The dotted/dashed black lines after 2015 show the projected trait change for the maximum (8.5) and minimum (2.6) IPCC carbon emission scenarios, respectively, from the HadGEM2 AO Global Circulation Model given the expected temperature change associated with those scenarios. Points along the left axis of each panel show the distribution of present-day community-weighted trait means per site (N = 117 sites) to better demonstrate the magnitude of projected change. Values are in original units (height = cm, LDMC = g/g, leaf area = cm^2, leaf nitrogen = mg/g, SLA = mm^2/mg).

Extended Data Fig. 8. Community trait co-variation is structured by temperature and moisture. a, Principal component analysis of plot-level community-weighted traits for seven key functional traits demonstrating how communities vary in multidimensional trait space. Trait correlations are highest between SLA and leaf nitrogen, and evergreenness and woodiness. Variation in SLA, leaf nitrogen, evergreenness and woodiness (PC1) are orthogonal to variation in height (PC2). Variation in leaf area and LDMC are explained by both PC 1 and 2. The color of the points indicates the soil moisture status of each plot at the site-level. **b-c,** Plot scores along PC axis 1, related to plant resource economy, vary with summer temperature, soil moisture, and their interaction (**b**) while plot scores along PC axis 2 vary only with soil moisture (**c**). The color of the points indicates the soil moisture of each site. Because not all plots and sites had woody species (and thus proportion evergreen could not be calculated) this analysis was conducted on a subset of 1098 (out of 1520) plots in 98 (out of 117) different sites.

Extended Data Figure 9. Temperature–trait relationships by growth form and site elevation. a, Mean (+/- SD) intraspecific temperature-height relationships (N = 80 species) per functional group. Dwarf shrubs are defined as those that do not grow above 30 cm in height (as estimated by regional floras: Flora of North America, USDA, Royal Horticultural Society, etc.) and are generally genetically limited in their ability to grow upright. There are no differences among functional groups in the magnitude of mean intraspecific temperature-height relationships. **b,** Relationship between community-weighted trait values, summer temperature, and soil moisture across biogeographic gradients, as in Fig. 2a. Points represent mean estimates per site (N = 117 sites) and are sized by the elevation of the site (larger circles = higher elevation). Ribbons represent the overall trait-temperature-moisture relationship (95% credible intervals on predictions at minimum and maximum soil moisture) across all sites.

Extended Data Table 1. Ecosystem functions influenced by each of the seven plant traits investigated.